

Journal of FOOD PROCESS ENGINEERING

**Edited by
D. R. HELDMAN**

**FOOD & NUTRITION PRESS, INC.
WESTPORT, CONNECTICUT 06880
USA**

VOLUME 6, NUMBER 3

QUARTERLY

JOURNAL OF FOOD PROCESS ENGINEERING

Editor: **D. R. HELDMAN**, Departments of Food Science and Human Nutrition and Agricultural Engineering, Michigan State University, East Lansing, Michigan.

Editorial Board: **A. L. BRODY**, Container Corporation of America, Oaks, Pennsylvania.

SOLKE BRUIN, Department of Food Science, Agricultural University, Wageningen, The Netherlands.

J. T. CLAYTON, Department of Food Engineering, University of Massachusetts, Amherst, Massachusetts.

J. M. HARPER, Agricultural and Chemical Engineering Department, Colorado State University, Fort Collins, Colorado.

C. G. HAUGH, Agricultural Engineering Department, Virginia Polytechnic and State University, Blacksburg, Virginia.

G. A. HOHNER, Quaker Oats Limited, Southhall, Middlesex, England.

C. J. KING, Department of Chemical Engineering, University of California, Berkeley, California.

D. B. LUND, Department of Food Science, University of Wisconsin, Madison, Wisconsin.

R. L. MERSON, Department of Food Science and Technology, University of California, Davis, California.

N. N. MOHSENIN, Consultation and Research, 120 Meadow Lane, State College, Pennsylvania.

R. P. SINGH, Agricultural Engineering Department, University of California, Davis, California.

All articles for publication and inquiries regarding publication should be sent to Prof. D. R. Heldman, Michigan State University, Department of Food Science and Human Nutrition, East Lansing, Michigan 48824 USA.

All subscriptions and inquiries regarding subscriptions should be sent to Food & Nutrition Press, Inc., 155 Post Road East, Suite 6, Westport, Connecticut 06880 USA.

One volume of four issues will be published annually. The price for Volume 6 is \$60.00 which includes postage to U.S., Canada, and Mexico. Subscriptions to other countries are \$72.00 per year via surface mail, and \$80.00 per year via airmail.

Subscriptions for individuals for their own personal use are \$40.00 for Volume 6 which includes postage to U.S., Canada, and Mexico. Personal subscriptions to other countries are \$52.00 per year via surface mail, and \$60.00 per year via airmail. Subscriptions for individuals should be sent direct to the publisher and marked for personal use.

The *Journal of Food Process Engineering* (ISSN 0145-8876) is published quarterly (March, June, September and December) by Food & Nutrition Press, Inc.—Office of Publication is 155 Post Road East, Suite 6, Westport, Connecticut 06880 USA. (current Issue is September 1982).

Second class postage paid at Westport, CT 06880.

POSTMASTER: Send address changes to Food & Nutrition Press, Inc., 155 Post Road East, Suite 6, Westport, CT 06880.

JOURNAL OF FOOD PROCESS ENGINEERING

JOURNAL OF FOOD PROCESS ENGINEERING

Editor:

D. R. HELDMAN, Departments of Food Science and Human Nutrition and Agricultural Engineering, Michigan State University, East Lansing, Michigan.

Editorial

A. L. BRODY, Container Corporation of America, Oaks, Pennsylvania.

Board:

SOLKE BRUIN, Department of Food Science, Agricultural University, Wageningen, The Netherlands.

J. T. CLAYTON, Department of Food Engineering, University of Massachusetts, Amherst, Massachusetts.

J. M. HARPER, Agricultural and Chemical Engineering Department, Colorado State University, Fort Collins, Colorado.

C. G. HAUGH, Agricultural Engineering Department, Virginia Polytechnic and State University, Blacksburg, Virginia.

G. A. HOHNER, Quaker Oats Limited, Southhall, Middlesex, England.

C. J. KING, Department of Chemical Engineering, University of California, Berkeley, California.

D. B. LUND, Department of Food Science, University of Wisconsin, Madison, Wisconsin.

R. L. MERSON, Department of Food Science and Technology, University of California, Davis, California.

N. N. MOHSENIN, Consultation and Research, 120 Meadow Lane, State College, Pennsylvania.

R. P. SINGH, Agricultural Engineering Department, University of California, Davis, California.

**Journal of
FOOD PROCESS ENGINEERING**

**VOLUME 6
NUMBER 3**

Editor: D. R. HELDMAN

**FOOD & NUTRITION PRESS, INC.
WESTPORT, CONNECTICUT 06880 USA**

© Copyright 1983 by
Food & Nutrition Press, Inc.
Westport, Connecticut USA

All rights reserved. No part of this publication may be reproduced, stored in a retrieval system or transmitted in any form or by any means: electronic, electrostatic, magnetic tape, mechanical, photocopying, recording or otherwise, without permission in writing from the publisher.

ISSN 0145-8876

Printed in the United States of America

CONTENTS

Use of Immobilized Lactase in Processing Cheese Whey Ultrafiltrate S. ROODPEYMA, C.G. HILL, Jr. and C.H. AMUNDSON , University of Wisconsin, Madison, Wisconsin	113
Error Analysis in Estimating Thermal Diffusivity from Heat Penetration Data JOHN W. LARKIN and JAMES F. STEFFE , Michigan State University, East Lansing, Michigan	135
Applicability of Flow Models with Yield for Tomato Concentrates M.A. RAO and H.J. COOLEY , Cornell University, Geneva, New York	159
Literature Abstracts	175

USE OF IMMOBILIZED LACTASE IN PROCESSING CHEESE WHEY ULTRAFILTRATE

S. ROODPEYMA,¹ C.G. HILL, JR.^{1,2} and C.H. AMUNDSON³

University of Wisconsin
Madison, WI 53706

Received for Publication January 13, 1982

ABSTRACT

*Enzymatic hydrolysis of lactose in cottage cheese whey ultrafiltrate was investigated. Lactase of *A. niger* was immobilized on an alumina-silica catalyst support by the linking agent tolylene-2, 4-diisocyanate. The resulting immobilized enzyme preparation had an activity of 3 standard international units of lactase per gram at pH 4 and 37°C. The optimum pH and temperature for hydrolysis of lactose by immobilized lactase were 3.5 and 50°C, respectively. Immobilization of the enzyme resulted in reductions of 1.1 pH units and 15°C in optimum pH and temperature, respectively.*

The two constants of the simple Michaelis-Menten rate expression were obtained from Lineweaver-Burk plots of the initial reaction rate data obtained at 37°C. Estimated values for V_{max} and the apparent K_m were 7.8 ($\mu\text{moles}/\text{min-g}$) and 0.26 (M), respectively.

Inhibition by the product galactose was measured by studying the hydrolysis reaction in a batch reactor. The inhibition constant K_i was estimated from batch reactor data to be 0.005 and 0.053 (M) at 35 and 50°C, respectively.

Activation energies of 8.1 and 6.4 (kcal/gmole) were obtained for the immobilized and soluble enzyme reactions, respectively.

The behavior of the batch reactor as measured in terms of a plot of conversion versus time was essentially the same for both conventional and deionized whey ultrafiltrate.

INTRODUCTION

Large quantities of cheese whey are produced every year in the United States. In 1976 alone about 34 billion pounds of liquid whey were produced with a concomitant production of more than 2 billion pounds of whey solids. Of this only 56.7% was further processed (Clark 1979).

¹ Department of Chemical Engineering, 1415 Johnson Drive

² Author to whom correspondence should be sent

³ Department of Food Science

Being rich in proteins and lactose, cheese whey has a high biological oxygen demand (BOD) of about 50,000 mg/1 (Knipschildt 1977). As a result, treatment of large quantities of whey as waste requires large sewage disposal plants with high operating costs. If the 34 billion pounds of whey produced in the U.S. in 1976 were treated in sewage disposal plants, the BOD would be equivalent to the sewage demand of 23 million people. The cost of building sewage plants for handling this load has been estimated at \$1 billion with an annual operating cost of \$39 million in 1976 dollars (McDonough 1977). One major aspect of this problem is due to lactose which is the most abundant component of whey solids (responsible for approximately 70% of its BOD (Shukla 1975)).

In recent years it has been discovered that a majority of the world's adult population is deficient in the enzyme lactase (Paige *et al.* 1971; Rosensweig 1969). The ingestion of large quantities of milk by these adults may lead to abdominal distress and diarrhea. Increasing the utility of milk, cheese whey and other dairy products by reducing the level of lactose in these nutritious food products has been the subject of intensive research in recent years. Such research activities are usually concerned with hydrolysis of the lactose in milk and whey. This hydrolysis can solve some of the problems associated with adding whey solids to food products.

This paper deals with the kinetics of the hydrolysis of lactose in cottage cheese whey ultrafiltrate and the deionized ultrafiltrate using an immobilized enzyme system comprised of β -galactosidase on alumina.

Lactases from bacterial (Hustad *et al.* 1973a,b; Ostergaard and Martiny 1973; Paine and Carlsonell 1975; Reagan *et al.* 1974; Wondolowski and Woychik 1974), fungal (Charles *et al.* 1974; Coughlin and Charles 1976; Coughlin *et al.* 1974; Hasselberger *et al.* 1974; Hyrkäs *et al.* 1976; Okos and Harper 1974; Okos *et al.* 1978; Olson and Stanley 1973; Paruchuri 1976; Pitcher *et al.* 1976; Weetall *et al.* 1974a,b; Wierzbicki *et al.* 1973; 1974; Woychik and Wondolowski 1972; 1973), and yeast (Dahlquist *et al.* 1973; Kilara *et al.* 1977; Pastore *et al.* 1974; 1976; Woychik *et al.* 1974) sources have previously been immobilized on a number of support materials and used in the hydrolysis of lactose present in different solutions. A fungal lactase derived from *A. niger* was used in this research. Use of covalent attachment via tolylene-2,4-diisocyanate for immobilization of the fungal lactase on alumina has not been reported elsewhere.

The present research includes studies of: (1) the pH and temperature profiles for the soluble and immobilized lactases; (2) initial reaction rates for the determination of kinetic parameters; and (3) batch reactor kinetics for evaluation of the galactose inhibition constant.

EXPERIMENTAL

Materials

Acid stable β -galactosidase derived from *Aspergillus niger* (Lactase N) was purchased from G.B. Fermentation Industries, Inc., Des Plaines, Illinois. The support for the preparation of the immobilized lactase was 1/4 in. solid spheres of silica- (17.9% w/w) alumina (80.3% w/w), catalog number SA-3232, supplied by Norton Chemical Process Products, Akron, Ohio. Its specific surface area was 30 m²/g. The laboratory chemicals used in this study were all reagent grade or better. Alfa-lactose monohydrate, gluco-stat reagents and glucose standard solution were obtained from Sigma Chemical Co., St. Louis, Missouri. Toluene-2,4-diisocyanate (TDI) and triethylamine were purchased from Aldrich Chemical Co., Milwaukee, Wisconsin.

Whey ultrafiltrate was prepared by passing cottage cheese whey through a plate and frame ultrafiltration apparatus obtained from the Water Technologies Division of Aqua Chem. Inc., Milwaukee, Wisconsin. The nominal molecular weight cutoff of the membranes employed was 30,000. The resulting permeate was subsequently spray dried and stored at 4°C. Ultrafiltrate solutions were reconstituted by dissolving appropriate amounts of the dried ultrafiltrate in a sodium acetate buffer (pH 4) or distilled water. Deionized ultrafiltrate was prepared by demineralization of the reconstituted ultrafiltrate in an ion exchange unit. The anion exchange resin (Ionac^R A-540, Strong Base) and the cation exchange resin (Dowex^R 50W-X8, Strong Acid) were obtained from the J. T. Baker Chemical Co., Phillipsburg, N.J.

Preparation of Buffer Solution

The buffer solution used throughout the immobilization and assay procedures was a stock solution containing 0.1 M sodium acetate, 1 mM EDTA, 1.5 mM MgSO₄, and 1.5 mM MnSO₄. The pH of the stock solution was decreased by addition of concentrated acetic acid or increased by addition of concentrated sodium hydroxide in order to adjust the pH to the desired level.

METHODS

Immobilization of Lactase

Lactase N was immobilized on the catalyst carriers by a procedure similar to the one used by Finocchiaro (1978). A series of experiments was carried out to establish the optimum levels of the principal factors

involved in the immobilization procedure. The experimental conditions employed were chosen on the basis of several fractional factorial designs (Box *et al.* 1978). These experiments established a strong preference for using a medium surface area support. They also indicated that the following immobilization procedure gave highest activity.

- a) Preparation of Support. A batch of the support (~5 g) was added to a crucible and activated by heating in a furnace at 500°C for 48 h. At the end of the activation period, the supports were removed from the furnace and cooled in a desiccator.
- b) Preparation of the Support-TDI (tolylene-2,4-diisocyanate) Complex. Five grams of heat-treated support were added to a 500 ml round bottom flask. This was followed by addition of 2 ml of TDI, 1 ml of triethylamine and 100 ml of freshly distilled acetone. The mixture was stirred for 2 h at room temperature and then the reaction solution was decanted from the support particles. These particles were then washed with dry acetone to remove excess TDI and dried and stored in a vacuum desiccator.
- c) Preparation of Support-TDI-Enzyme Complex. Five grams of derivatized support particles were added to 50 ml of enzyme solution [5 mg/ml in the sodium acetate buffer (pH 4.0)] in a large test tube. The reaction mixture was shaken at 28 cycles/min on a wrist action shaker at room temperature for 2 h. Shaking was then continued overnight at 4°C. Immobilized enzyme preparations were washed with the buffer (approximately 300 ml/5 g support) and then stored in the buffer (pH 4.0) at 4°C.

Determination of Lactase Activity

The activity of a preparation of β -galactosidase can be estimated using lactose as substrate by measuring the amount of glucose which is produced in a specified period of time. The activity is quantified in terms of standard international units of lactase which we shall term lactase units (LU) per gram of enzyme, where (LU) is the number of micromoles of glucose liberated in one minute under specified reaction conditions (pH and temperature).

A 0.8 M lactose solution in the sodium acetate buffer was used for determination of the activities of both soluble and bound enzyme.

For the soluble lactase activity determinations, 100 μ l of a 5 mg/ml solution of the enzyme (Lactase N) in the sodium acetate buffer (pH 4.0) was added to 20 ml of the substrate lactose solution. The reaction mixture was shaken at 100 oscillations/min for 15 min. Throughout the experiment liquids were maintained at 37°C. The reaction was stopped by removing a 1.0 ml aliquot from the reaction mixture and placing it

in a boiling water bath for 3 min. This procedure was quite effective in quenching the reaction via enzyme deactivation. Both the soluble and the immobilized forms of lactase quickly lose all activity in the 70-80°C range. The amount of additional lactase hydrolysis which occurred during the heating period was within the expected error for the experiment.

In the case of immobilized lactase (IML), 4 pieces of IML preparation, which had been stored at 4°C in the sodium acetate buffer (pH 4.0), were placed on absorbent tissue paper to remove excess buffer. The pieces were immediately weighed (the weight ranged from 0.8 to 1.1 g) and added to a test tube containing 1.0 ml of the buffer solution (pH 4.0). This test tube and one containing the substrate solution were immersed for 15 minutes in a bath maintained at 37°C. The reaction was started by adding the contents of the test tube to the substrate solution. The procedure for the soluble enzyme was then followed.

The immobilized lactase preparation was analyzed twice a week for activity over a period of four months. No significant decline in activity was noted for the storage conditions employed (4°C). Deactivation during use, however, can be expected to depend on the operating conditions employed.

The glucose concentration was determined by the Sigma Glucostat Method (1978). The procedure involved adding 5 ml of an appropriately diluted assay solution and holding the mixture at room temperature for 45 min. The absorbance of this mixture at 450 nm was determined using a Beckman Model 25 Spectrophotometer. Standards were prepared using β -D-Glucose solutions of known concentration.

Determination of Initial Reaction Rate

In order to calculate the Michaelis-Menten constants for hydrolysis of lactose by immobilized lactase, initial reaction rates were determined for different levels of the initial substrate concentration. This was accomplished by following the assay procedure for immobilized lactase discussed above, except that for each assay, three 1.0 ml samples were removed from the reaction mixture at times 1, 2 and 5 min from the start of the reaction. Each sample vial was kept in a boiling water bath for 3 min to quench the reaction. The glucose concentration in each sample was then determined.

Batch Reactor Experiments

In order to study the reaction over an extended period of time, the extent of reaction was determined at various times in a batch reactor. In a typical run, 100 ml of a substrate solution was first prepared. The

substrate solution was a 0.2 M solution of lactose in the sodium acetate buffer (pH 4) or a solution of dried permeate in the buffer or distilled water or a batch of the deionized permeate prepared by the ion exchange operation. The flask containing the substrate solution and another flask containing 10 g of immobilized lactase in 5 ml of the buffer solution were kept in an incubator for approximately 15 min to bring their temperatures to the desired level.

At time zero, the contents of the flask of immobilized lactase were added to the substrate solution. Then small samples (0.5 ml) of the reaction mixture were taken at different times over a 12 to 14 h period. Each sample vial was immediately immersed in a boiling water bath and kept there for 3 min to deactivate any enzyme that might have been released from the immobilized enzyme preparation. The concentration of glucose in each sample was then determined.

RESULTS AND DISCUSSION

Activity of Soluble and Immobilized Lactase

The activity of the soluble lactase measured at its optimum reaction conditions (pH 4.6 and 65°C) was 8760 (LU/g). Similarly, an activity of 8.9 LU/g was obtained for the immobilized lactase at its optimum reaction conditions (pH 3.5 and 50°C).

pH Profile

As a first step in finding the best set of conditions for maximum reaction rate, the pH profiles of the immobilized and soluble lactase were determined. This was accomplished by measuring the activity of each lactase in substrate solutions of various pH levels (ranging from 3 to 6) at a constant temperature (37°C) (see Fig. 1). The immobilized lactase preparation showed maximum activity at pH 3.5. Immobilization of lactase reduces its optimum pH by 1.1 units. In each case the activity is normalized relative to the maximum activity of the enzyme in question.

Temperature Profile and Activation Energy

The temperature profiles of both soluble and immobilized lactase were determined by measuring their activities in the lactose solution at several temperatures (ranging from 40 to 70°C) and a constant pH of 4. These temperature profiles are shown in Fig. 2. In each case enzyme activity is normalized relative to the maximum for the enzyme form in question. The activity of the soluble lactase increases with temperature

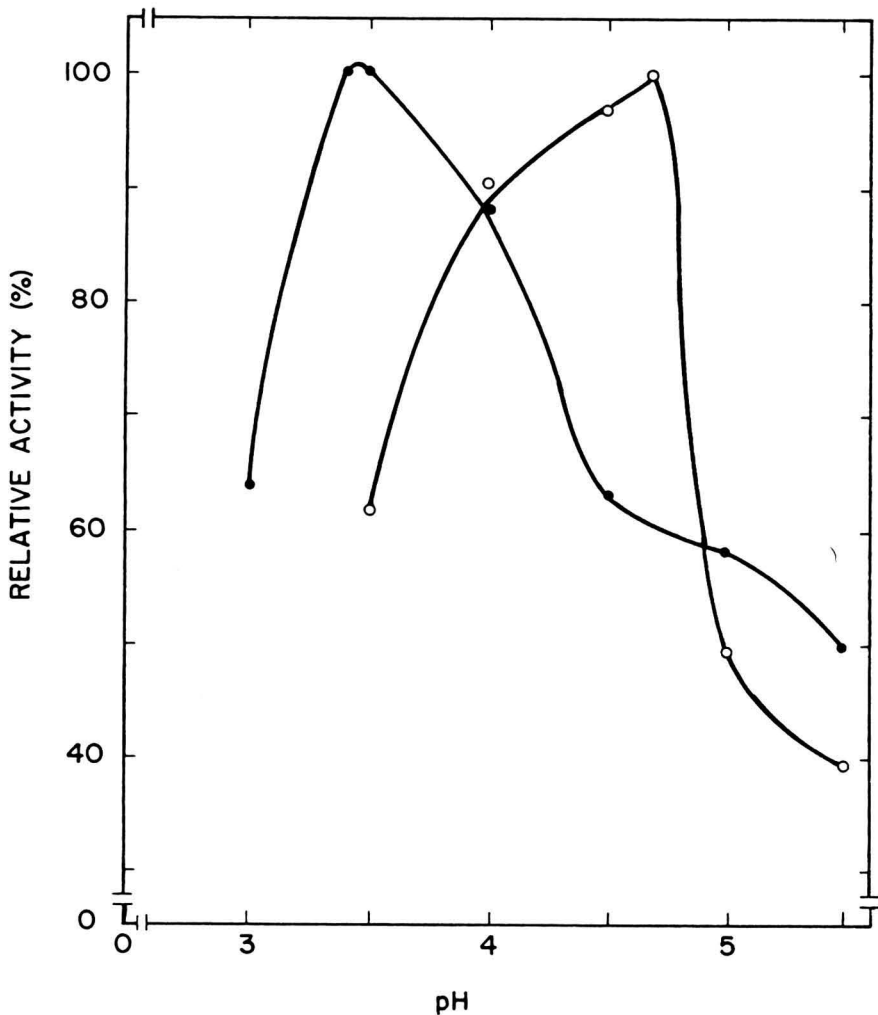


FIG. 1. EFFECT OF ASSAY pH ON THE ACTIVITY OF LACTASE AT 37°C, (●), IMMOBILIZED LACTASE; (○), SOLUBLE LACTASE

Relative activity is activity at each temperature divided by maximum activity ($3.8 \mu\text{moles glucose/min-g}$ for the immobilized lactase and $8760 \mu\text{mole glucose/min-g}$ for the soluble lactase).

up to 65°C , whereas the activity of the immobilized lactase drops sharply after 50°C , so that at 65°C it has virtually no activity. Therefore, the optimum temperature of the lactase decreases by 15°C upon immobilization. The shifts in optimum temperature and pH of enzymes as a result of their immobilization are usually attributed to structural modification of the enzyme and/or a change in its microenvironment.

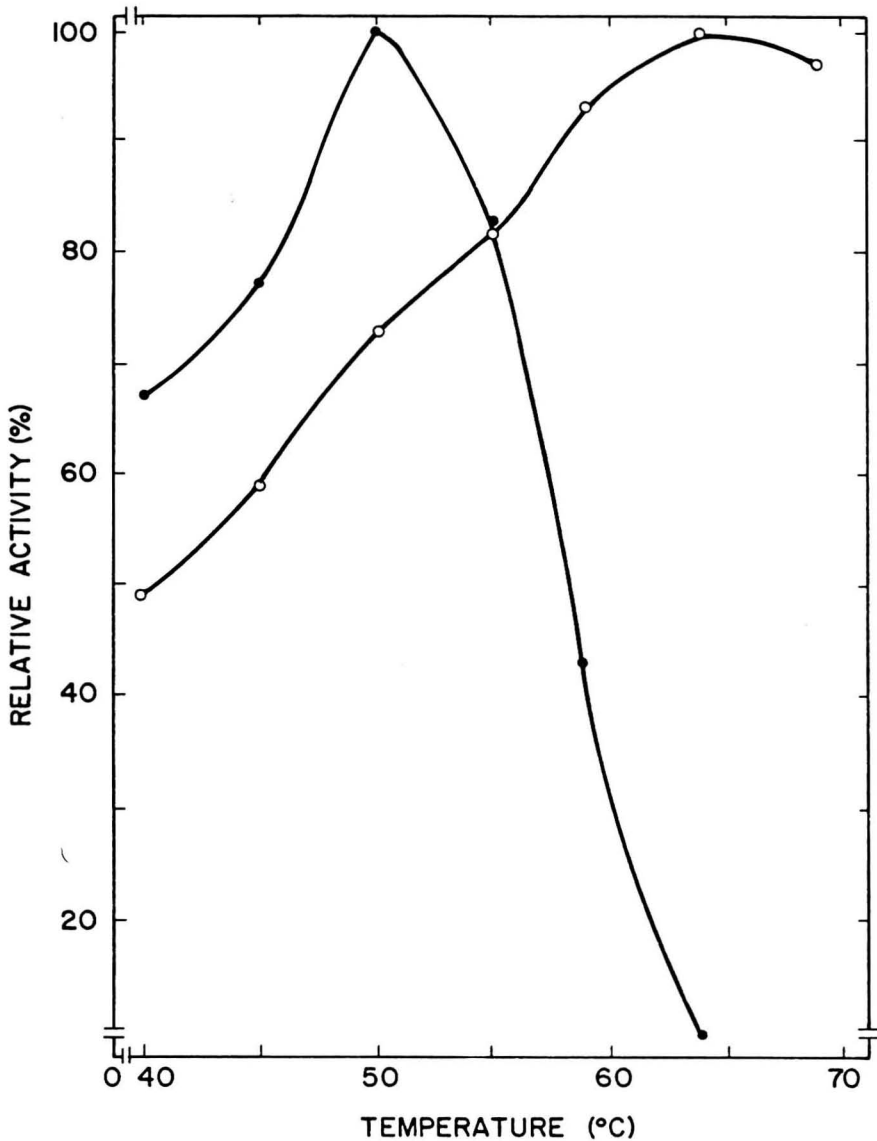


FIG. 2. EFFECT OF ASSAY TEMPERATURE ON THE ACTIVITY OF LACTASE AT pH 4, (●), IMMOBILIZED LACTASE, (○), SOLUBLE LACTASE
Relative activity is activity at each temperature divided by maximum activity ($8.9 \mu\text{moles glucose/min-g}$ for the immobilized lactase and $4250 \mu\text{moles glucose/min-g}$ for the soluble lactase).

A semilog plot of the relative activity versus reciprocal temperature was fitted to a straight line. From the slope of this line (Fig. 3), the activation energies were calculated as 6.4 and 8.1 (kcal/gmole) for the soluble and immobilized lactase, respectively.

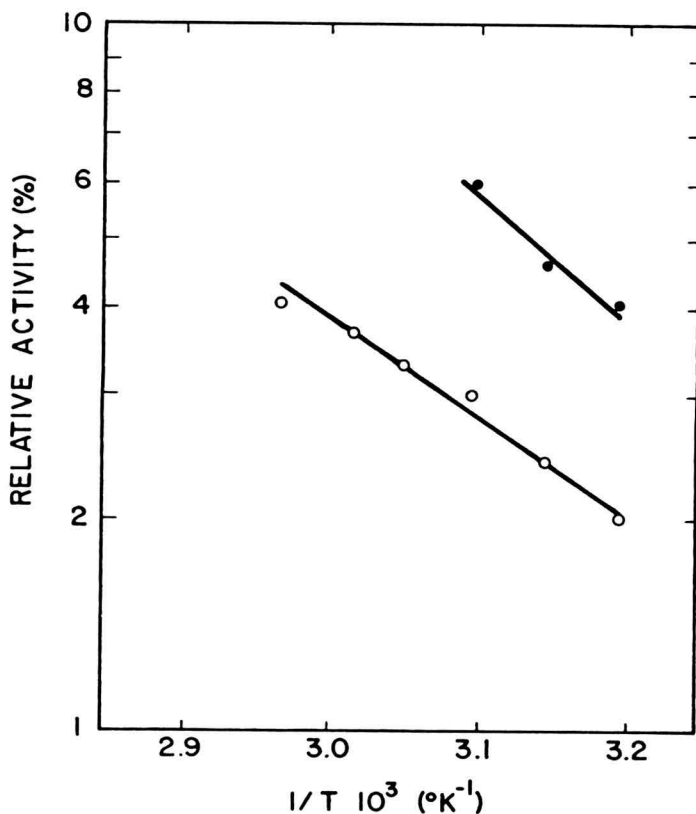


FIG. 3. ARRHENIUS PLOTS, (●), IMMOBILIZED LACTASE; (○) SOLUBLE LACTASE

Determination of Michaelis-Menten Constants from Initial Rate Measurements

In order to check the adequacy of the Michaelis-Menten rate expression for hydrolysis of lactose by the immobilized lactase preparation, initial reaction rates were determined at several levels of initial substrate concentration. Lactose solutions in the sodium acetate buffer (pH 4.0) were used as substrate. All initial rates were determined at 37°C. Each initial rate was determined from the slope of the straight line corresponding to the plot of glucose concentration versus time for a five minute period at the start of reaction. The experimental run at each level of substrate concentration was replicated. Typical straight line plots are shown in Fig. 4.

Next, a Lineweaver-Burk plot was prepared by plotting the reciprocal of the initial rate against the reciprocal of the substrate concentration. (See Fig. 5.) A weighted least squares analysis (Box *et al.* 1978)

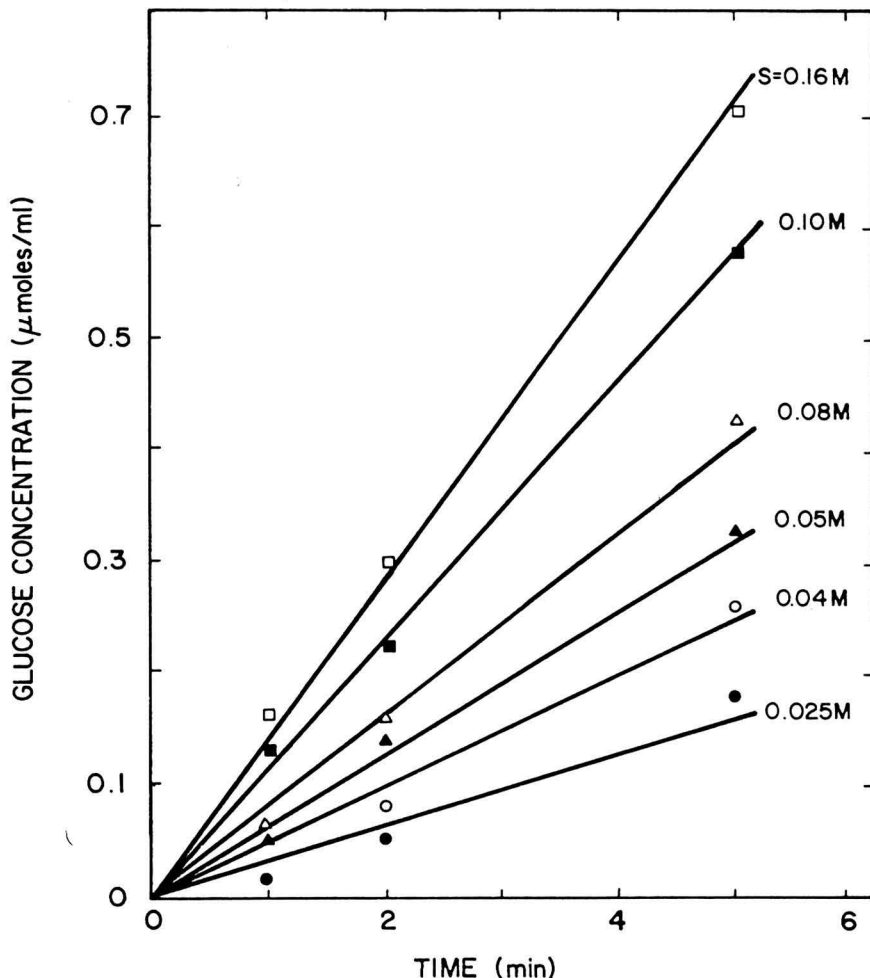


FIG. 4. GLUCOSE CONCENTRATION PLOTTED AGAINST TIME FOR DETERMINATION OF INITIAL RATE, S = SUBSTRATE CONCENTRATION (37°C)

was used in fitting the reciprocal plot to a straight line. The Michaelis-Menten rate constants, V_{\max} and the apparent K_m were calculated from the slope and intercept of the straight line. The resulting estimates for the rate constants are $7.85 \pm 2.64 \mu\text{moles}/\text{min-g}$ and $0.263 \pm 0.090 \text{ M}$, respectively.

Determination of K_m and K_i from Batch Reactor Experiments with Lactose Solutions

In order to study the hydrolysis reaction over extended periods of time, several experimental runs were carried out in a batch reactor. At

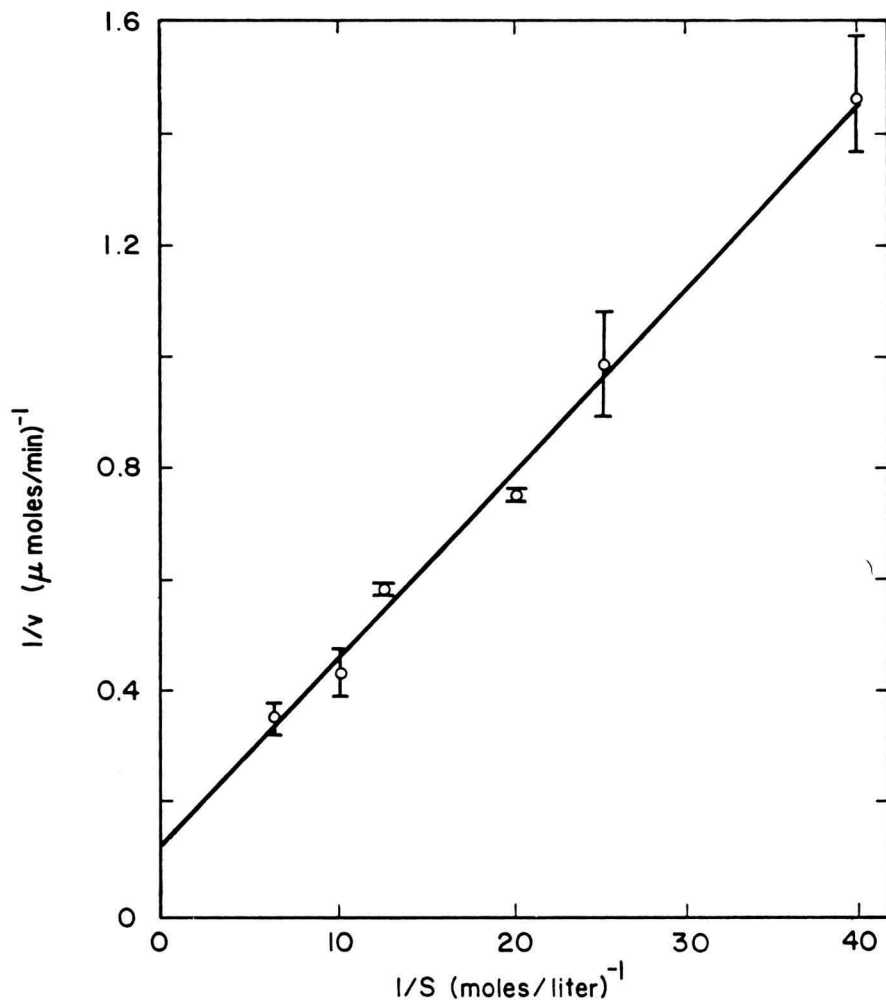


FIG. 5. THE LINEWEAVER-BURK PLOT FOR HYDROLYSIS OF LACTOSE BY IMMOBILIZED LACTASE (37°C)

long times galactose accumulates to the point that its inhibitory effects on the enzyme can no longer be neglected (Weetall *et al.* 1974b; Woychik and Wondolowski 1972). In this case, it is necessary to use the following version of the Michaelis-Menten rate expression

$$v = \frac{kES/V_R}{S + K_m[1 + (P/K_i)]} \quad (1)$$

where v = reaction rate
 k = rate constant
 E = amount of enzyme
 V_R = volume of substrate solution
 kE/V_R = V_{\max} (the maximum rate achieved when $S \gg K_m$)
 S = substrate concentration
 K_m = Michaelis constant
 p = product concentration
 and K_i = inhibition constant

Equation (1) can be integrated from time zero to time t to obtain the following design expression for a batch reactor (assuming that no product is present initially and that reaction of 1 mole of lactose yields 1 mole of glucose plus 1 mole of galactose).

$$(kE/V_R S_0)t = [1 - (K_m/K_i)]f + K_m(1/K_i + 1/S_0)\ln[1/(1 - f)] \quad (2)$$

t = elapsed time
 S_0 = initial substrate concentration
 f = $(S_0 - S) / S_0$ = fraction conversion at time t

This equation can be rewritten in the following form:

$$y = a_1 x_1 + a_2 x_2 = Ct \quad (3)$$

where

$$\begin{aligned} C &= kE/V_R S_0 & a_1 &= 1 - [K_m/K_i] \\ x_1 &= f & a_2 &= K_m(1/K_i + 1/S_0) \\ x_2 &= \ln[1/(1 - f)] \end{aligned}$$

The parameter V_{\max} was first determined from measurements of the initial rate in a concentrated (25% w/w) lactose solution at 50 and at 35°C. Then the glucose concentration versus time data generated in batch reactor runs with 0.2 M lactose solutions at 50 and 35°C were correlated according to Eq. (3) by the method of regression analysis to determine the two coefficients a_1 and a_2 . Subsequent manipulations of these parameters lead to values of two constants K_m and K_i . The resulting estimates for the apparent K_m and K_i are presented in Table 1. The experimental data are shown in Fig. 6 together with the curves calculated from the best fit parameters.

In order to examine the possibility of utilizing the immobilized lactase with a concentrated substrate solution, a batch reactor experiment was carried out with a 0.8 M lactose solution at 50°C. The

Table 1. Parameters of the Michaelis-Menten rate expression for the immobilized enzyme

Parameter	Estimate	Standard Error
V_{\max}^a ($\mu\text{moles}/\text{min-g}$)	7.85	± 2.64
K_m^a (M)	0.26	± 0.09
V_{\max}^b ($\mu\text{moles}/\text{min-g}$)	8.86	± 1.14
V_{\max}^c ($\mu\text{moles}/\text{min-g}$)	4.81	
K_m^d (M)	0.028	± 0.093
K_i^d (M)	0.0046	± 0.016
K_m^e (M)	0.110	± 0.11
K_i^e (M)	0.053	± 0.061
K_m^f (M)	1.92	± 0.57
K_i^f (M)	0.63	± 0.28

^a Estimated from initial rate measurements at 37°C.

^b Estimated from activity measurement in 25% lactose solution at 50°C.

^c Estimated from activity measurement in 25% lactose solution at 35°C.

^d Estimated from batch reactor data at 35°C with 0.2 M lactose solution.

^e Estimated from batch reactor data at 50°C with 0.2 M lactose solution.

^f Estimated from batch reactor data at 50°C with 0.8 M lactose solution.

resulting data (plotted in Fig. 7 together with the data for the 0.2 M solution at 50°C) were correlated on the basis of Eq. (3). Estimates of 1.92 ± 0.57 M and 0.63 ± 0.28 M were obtained for the apparent K_m and K_i , respectively. These values are one to two orders of magnitude higher than those obtained with the 0.2 M lactose solution. These results indicate that while a conversion of at least 70% can be achieved with the concentrated substrate, the values of the kinetic parameters that were determined with the dilute substrate solution are not applicable to the concentrated solution.

Nevertheless, the possibility of using the same values for the apparent K_m and K_i that were determined with the 0.2 M lactose solution for expressing the time dependence of fraction conversion for the concentrated solution was checked. Since K_i is approximately two orders of magnitude smaller than S_0 (when S_0 varies between 0.1 and 0.9 M) the term $1/S_0$ on the right side of Eq. (2) can be neglected. Therefore, the relation between percent conversion and the combined variable t/S_0 is *approximately* the same for various values of S_0 . The batch reactor data of both solutions were plotted in the form of percent conversion against the ratio of time to initial substrate concentration (see Fig. 8).

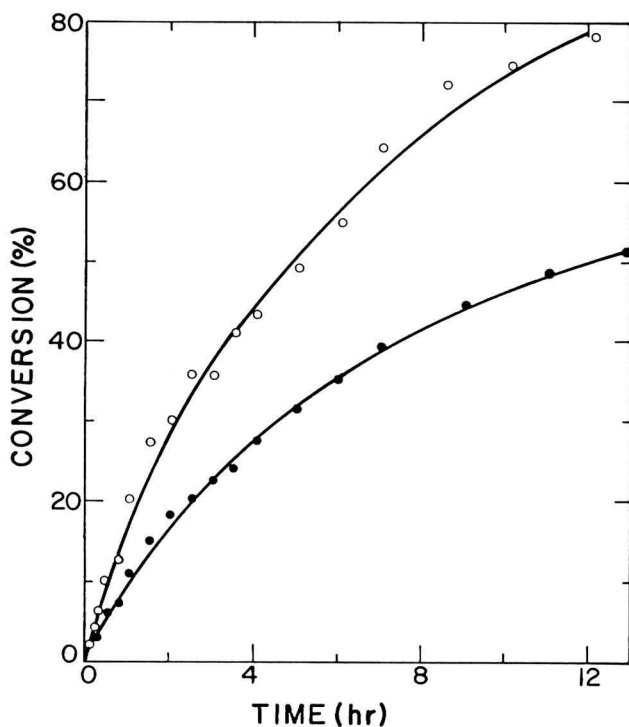


FIG. 6. BATCH REACTOR DATA WITH 0.2 M LACTOSE SOLUTION, (○), 50°C; (●), 35°C

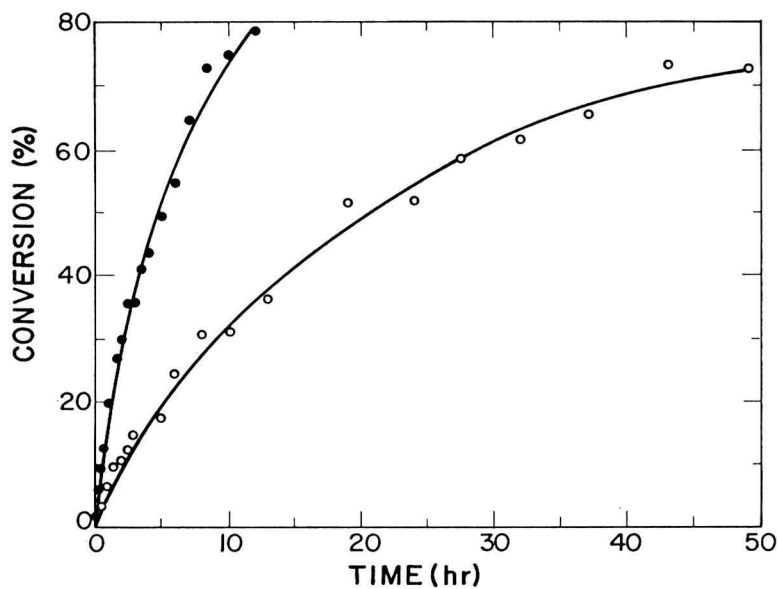


FIG. 7. BATCH REACTOR DATA WITH LACTOSE SOLUTIONS AT 50°C, (●), 0.2 M; (○) 0.8 M

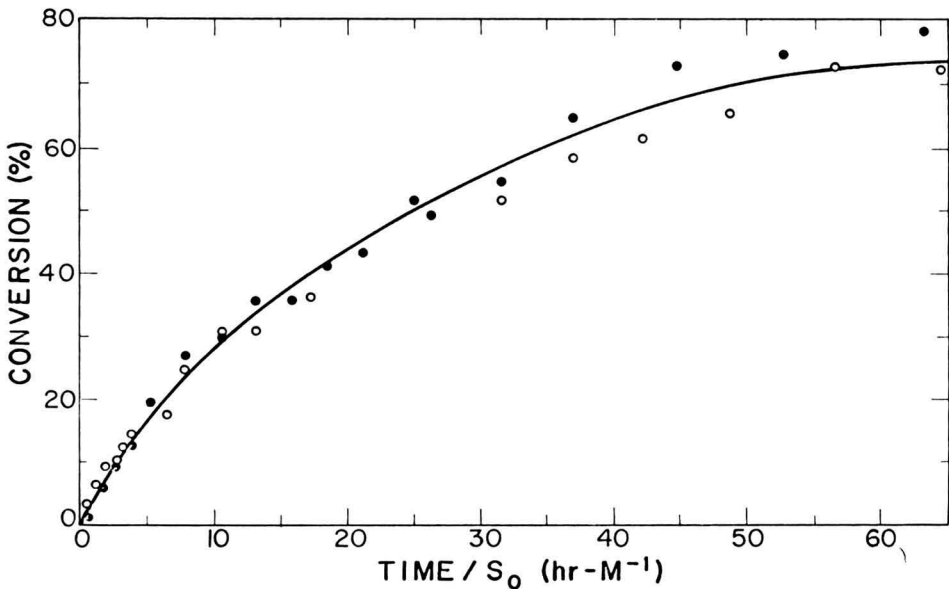


FIG. 8. BATCH REACTOR DATA WITH LACTOSE SOLUTION AT 50°C PLOTTED AS CONVERSION VERSUS t/S_0 , (●), 0.2 M; (○), 0.8 M

The data points of the two runs lie close to the same graph, especially at lower levels of conversion, indicating that the values of K_m and K_i , obtained with the dilute substrate solution, may be used with caution for extrapolating the batch reactor data to more concentrated lactose solutions.

Another batch reactor run with the 0.8 M lactose solution made over a 12 h period (in which 40% conversion was achieved) produced similar results.

Hydrolysis of Lactose in Whey Ultrafiltrate and Deionized Permeate

In order to study the influence of ash on the kinetics of lactose hydrolysis, experimental runs were carried out (at 50°C) using both whey ultrafiltrate permeate and deionized permeate as substrate. The deionized permeate solution was obtained by ion exchange. Minute amounts of concentrated acetic acid were used to adjust the pH of the deionized permeate from 7 to 4. The whey ultrafiltrate was prepared by dissolving the dried permeate in distilled water (resulting in pH 5.5) or in sodium acetate buffer (pH 4.0). The concentration of lactose in the solution was equivalent to that of the deionized permeate (0.14 M). The experimental data are plotted as percent conversion versus time in Fig. 9. Four experimental runs comprised of two runs with the deionized

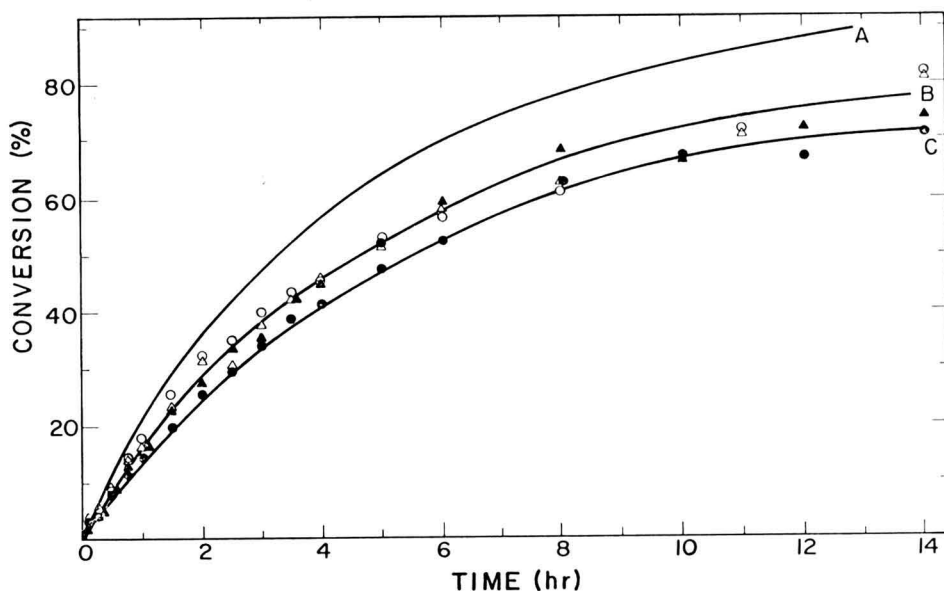


FIG. 9. BATCH HYDROLYSIS OF LACTOSE AT 50°C

- (○), whey ultrafiltrate prepared with pH 4 buffer, (curve B);
- (△) deionized permeate, pH adjusted to 4, (curve B);
- (●), whey ultrafiltrate prepared with distilled water, (curve C);
- (▲), deionized permeate, no pH adjustment, (curve B);
- solid line, theoretical curve for 0.14 M lactose (curve A).

permeate (before and after pH adjustment) and two runs with the nondeionized permeate (dissolved in water and in the pH 4 buffer) were carried out. Except for the points corresponding to the run with the nondeionized permeate solution prepared with distilled water (curve C), all the experimental points lie on the same curve (curve B). Curve A in Fig. 9 (drawn for purposes of comparison) is the curve calculated for a 0.14 M lactose solution. The experimental data obtained with the two substrates (at pH 4) were fitted on the basis of the linear model (Eq. 3) and values for the apparent K_m and K_i were calculated. The same value of V_{max} that was used in analysis of the data for the lactose solutions was used in these calculations. The results are presented in Table 2.

The values for the apparent K_m and K_i obtained with the two substrates are almost the same. Therefore, demineralization of the permeate does not seem to affect the performance of a batch reactor. Furthermore, adjustment of the pH of the deionized permeate does not influence the batch hydrolysis of lactose but use of the pH 4 buffer solution (instead of water) for reconstitution of the nondeionized

Table 2. Michaelis-Menten constants determined with substrates other than lactose

Parameter	Estimate	Standard Error
K_m^a (M)	0.146	± 0.099
K_i^a (M)	0.040	± 0.032
K_m^b (M)	0.142	± 0.111
K_i^b (M)	0.038	± 0.036

^a Deionized permeate used as substrate.

^b Whey ultrafiltrate used as substrate.

The standard errors for estimates from initial rate data are based on genuine replications but the standard errors reported for K_m and K_i (calculated from batch reactor data) are obtained from the total residual sum of squares as described by Box, *et al.* (1978).

permeate solution slightly improves batch reactor performance. The large deviation of the theoretical graph from the calculated curve is attributed to inhibition by some of the constituents of the permeate (other than the mineral salts).

Hydrolysis of Whey Ultrafiltrate at Different Levels of the Ratio of Solution Volume to Enzyme Weight.

In order to experimentally determine the effect of changing the ratio of solution volume (V_R) to enzyme weight (E), three runs were carried out using a permeate solution (with an equivalent lactose concentration of 0.2 M) at 50°C. The solution was prepared by dissolving an appropriate amount of dried permeate in sodium acetate buffer (pH 4). The amounts of substrate solution used were 60, 100 and 140 ml. The same amount of immobilized lactase (~ 10 gr) was used in the three runs. The resulting data are plotted as percent conversion versus time in Fig. 10.

The effects of the amount of enzyme and the volume of the reaction mixture on the behavior of a batch reactor can be combined so that their ratio can be treated as a single variable. This can be seen by looking at the integrated design equation for a batch reactor. In general form, the design equation can be written as:

$$-\frac{dS}{dt} = \frac{kE}{V_R} \phi(S) \quad (4)$$

where

$\phi(S)$ = a general function expressing the dependence of the rate of reaction on substrate concentration

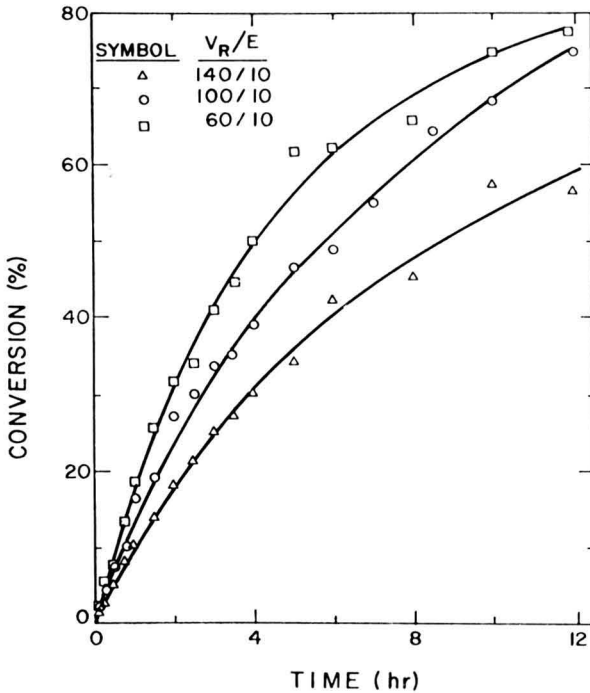


FIG. 10. BATCH HYDROLYSIS OF LACTOSE IN PERMEATE AT 50°C
Data plotted as conversion versus time at various levels of V_R/E .

Integrating over the period of reaction time, t :

$$(kE/V_R)t = - \int_{S_0}^S dS/\phi(S) = \psi(S) \quad (5)$$

The right hand side of this equation [$\psi(S)$] is constant for a fixed level of conversion. Combining this constant with k and denoting the combined group by A , we can rewrite Eq. (5) as:

$$t = (V_R/E)A \quad (6)$$

This equation indicates that the percent conversion versus time data obtained at different levels of the ratio V_R/E , must fall on the same curve if plotted as percent conversion against $t E/V_R$.

In order to check the adherence of the data to Eq. (6), they were plotted as percent conversion versus the combined variable $t V_R/E$ as shown in Fig. 11. The experimental data points of the three runs tend to lie close to the same curve (the solid line in Fig. 11) although some scatter is observed, especially at high levels of conversion.

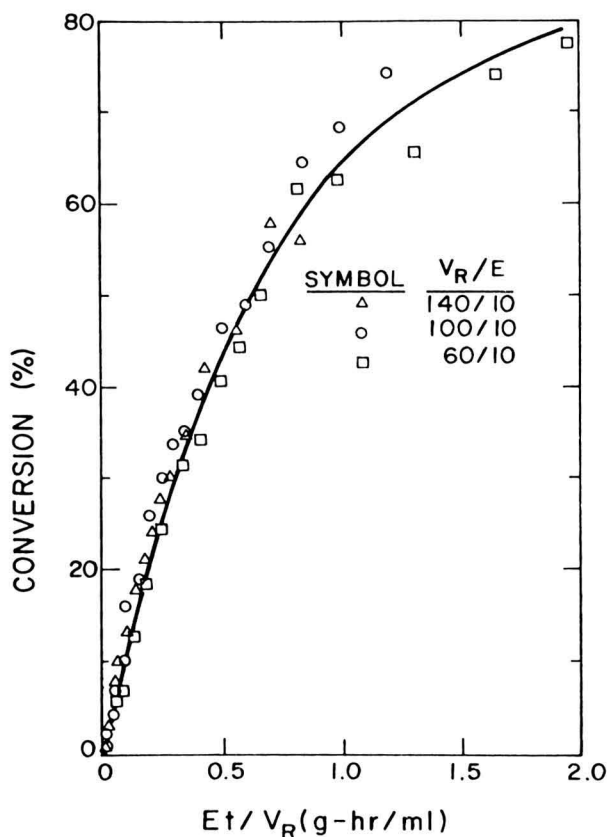


FIG. 11. BATCH HYDROLYSIS OF LACTOSE IN PERMEATE AT 50°C
Data plotted as conversion versus Et/V_R at various levels of V_R/E .

CONCLUSIONS

Lactase of *A niger* immobilized on silica-alumina with tolylene-2, 4-diisocyanate as a linking agent has maximum activity at a pH of 3.5 and a temperature of 50°C. For the hydrolysis of lactose the Michaelis-Menten parameters V_{max} and K_m were determined via initial rate measurements at 37°C to be 7.8 ± 2.6 ($\mu\text{moles}/\text{min-g}$) and 0.26 ± 0.09 (M), respectively. V_{max} was also determined by measurement of the activity of the immobilized lactase in a concentrated (25% w/w) lactose solution. The values obtained at 35 and 50°C were 4.8 and 8.9 ($\mu\text{moles}/\text{min-g}$), respectively.

Batch reactor studies with elevated lactose concentrations were also used to evaluate the Michaelis-Menten parameters and the inhibition constant for galactose. Additional batch reactor studies with the

permeate produced by ultrafiltration of cottage cheese whey indicated that conversions approaching 80% could be achieved. Demineralization of this permeate prior to hydrolysis did not have a significant effect on the observed kinetics.

ACKNOWLEDGMENTS

This research was supported in part by funds from the Wisconsin Alumni Research Foundation. Equipment donations from Aqua Chem Inc. greatly facilitated the present work. One of us (S.R.) is indebted to the University of Wisconsin Research Committee and the Walter B. Schulte Trust Fund for Financial aid in the form of a Research Assistantship and Scholarship Prize Funds, respectively.

REFERENCES

- Anonymous. 1978. The enzymatic colorimetric determination of glucose. Sigma Chemical Co., St. Louis, Missouri.
- BOX, G.E.P., HUNTER, W.G. and HUNTER, J.S. 1978. Statistics for experimenters. John Wiley & Sons, New York.
- CHARLES, M., COUGHLIN, R.W., ALLEN, B.R., PARUCHURI, E.K. and HASSELBERGER, F.X. 1974. Lactase immobilized on stainless steel and other dense metal and metal oxide supports. *Adv. Exp. Med. Biol.* 42, 213.
- CLARK, W.S., JR. 1979. Major whey products markets—1976. *J. Dairy Sci.* 62, 96.
- COUGHLIN, R.W. and CHARLES, M. 1976. Conversion of cheese whey waste into valuable products using immobilized enzymes in fluidized bed reactors. In *Enzyme Technology Grantees-Users Conference*, (E.K. Pye, ed.) 107 pp, University of Pennsylvania Press, Philadelphia, PA.
- COUGHLIN, R.W., CHARLES, M., ALLEN, B.R., PARUCHURI, E.K. and HASSELBERGER, F.X. 1974. Increasing economic value of whey wastewater using immobilized lactase. *AICHE Symposium Series I: Water-Industrial Waste Treatment.* 199 pp.
- DAHLQUIST, A., MATTIASSON, B. and MOSBACH, K. 1973. Hydrolysis of β -galactosidase using polymer-entrapped lactase. A study towards producing lactose-free milk. *Biotechnol. Bioeng.* 15, 395.
- FINOCCHIARO, E.T. 1978. Lactase immobilized on inorganic supports for the continuous hydrolysis of lactose. M.S. Thesis, University of Wisconsin.
- HASSELBERGER, F.X., ALLEN, B., PARUCHURI, E.K., CHARLES, M. and COUGHLIN, R.W. 1974. Immobilized enzymes: lactase bond-

- ed to stainless steel and other dense carriers for use in fluidized bed reactors. *Biochem. Biophys. Res. Commun.* 57, 1054.
- HUSTAD, G.O., RICHARDSON, T. and OLSON, N.F. 1973a. Immobilization of β -galactosidase on an insoluble carrier with a polyisocyanate polymer. Part I: preparation and properties. *J. Dairy Sci.* 56, 1111.
- HUSTAD, G.O., RICHARDSON, T. and OLSON, N.F. 1973b. Immobilization of β -galactosidase on an insoluble carrier with a polyisocyanate polymer. Part 2: kinetics and stability. *J. Dairy Sci.* 56, 1118.
- HYRKÄS, K., VISKARI, R., LINKO, Y.Y. and LINKO, M. 1976. Hydrolysis of lactose in acid whey by immobilized β -galactosidase. *Milchwissenschaft* 31, 129.
- KILARA, A., SHAHANI, K.M. and WAGNER, F.W. 1977. Preparation and characterization of immobilized lactase. *Lebensm.-Wiss. Technol.* 10, 84.
- KNIPSCHILDT, M.E. 1977. Utilization of whey to avoid pollution and to recover a valuable food product. *Am. Dairy Rev.* 39, 52B.
- MCDONOUGH, F.E. 1977. Whey solids utilization and salvage systems. *Cult. Dairy Prod. J.* 12, 8.
- OKOS, M.R., GRULKE, E.A. and SYVERSON, A. 1978. Hydrolysis of lactose in acid whey using β -galactosidase adsorbed to a phenol formaldehyde resin. *J. Food Sci.* 43, 566.
- OKOS, E.S. and HARPER, W.J. 1974. Activity and stability of β -galactosidase immobilized on porous glass. *J. Food Sci.* 39, 88.
- OLSON, A.C. and STANLEY, W.L. 1973. Lactase and other enzymes bound to a phenol formaldehyde resin with glutaraldehyde. *J. Agric. Food Chem.* 21, 440.
- OSTERGAARD, J.C.W. and MARTINY, S.C. 1973. The immobilization of β -galactosidase E.C.-3.2.1.23 through encapsulation in water insoluble microcapsules. *Biotechnol. Bioeng.* 15, 561.
- PAIGE, D.M., BAYLESS, T.M., FERRY, G.C. and GRAHAM, G.C. 1971. Lactose malabsorption and milk rejection in negro children. *Johns Hopkins Med. J.* 129, 163.
- PAINE, M.A. and CARLSONELL, R.G. 1975. Immobilization of β -galactosidase E.C.3.2.1.33 in bolladion microcapsules. *Biotechnol. Bioeng.* 17, 617.
- PARUCHURI, E.K. 1976. Hydrolysis of lactose in acid whey using immobilized lactase. Ph.D. Dissertation, Lehigh University.
- PASTORE, M., MORISI, F. and VIGLIA, A. 1974. Reduction of lactose content of milk with entrapped β -galactosidase. II. Suitable conditions for an industrial continuous process. *J. Dairy Sci.* 57, 269.
- PASTORE, M., MORISI, F. and LEALI, L. 1976. Reduction of lactose of milk by entrapped β -galactosidase. IV: Results of long-term experiments on pilot plant. *Milchwissenschaft* 31, 362.
- PITCHER, W.H., JR., FORD, J.R. and WEETALL, H.H. 1976. The preparation, characterization and scale-up of a lactase system immobilized to inorganic supports for the hydrolysis of acid whey. In

- Methods in enzymology: Immobilized enzymes.* 792 pp. (K. Mosbach, ed.) Academic Press, New York.
- REAGAN, D.L., DUNNILL, P. and LILLY, M.D. 1974. Immobilized enzyme reaction. Stability attrition of the support material. *Biotechnol. Bioeng.* 16, 333.
- ROSENSWEIG, N.S. 1969. A review of dietary lactose and its varied utilization by man. A publication of the Whey Products Institute.
- SHUKLA, T.P. 1975. Beta-galactosidase technology: A solution to the lactose problem. *CRC Crit. Rev. Food Technol.* 5, 325.
- WEETALL, H.H., HAVEWALA, N.B., PITCHER, W.H., JR, DETAR, C.C., VANN, W.P. and YAVERBAUM, S. 1974. Preparation of immobilized lactase. Continued studies on the enzymic hydrolysis of lactose. *Biotechnol. Bioeng.* 16, 689.
- WEETALL, H.H., HAVEWALA, N.B., PITCHER, W.H., JR, DETAR, C.C., VANN, W.P. and YAVERBAUM, S. 1974a. Preparation of immobilized lactase. Continued studies on the enzymic hydrolysis of lactose. *Biotechnol. Bioeng.* 16, 689.
- WIERZBICKI, L.E., EDWARDS, V.H. and KOSIKOWSKI, F.V. 1973. Immobilization of microbial lactases by covalent attachment to porous glass. *J. Food Sci.* 38, 1070.
- WIERZBICKI, L.E., EDWARDS, V.H. and KOSIKOWSKI, F.V. 1974. Hydrolysis of lactose in acid whey using β -galactosidase immobilized on porous glass particles. Preparation and characterization of a reusable catalyst for the production of low-lactose dairy products. *Biotechnol. Bioeng.* 16, 397.
- WONDOLOWSKI, M.V. and WOYCHIK, J.H. 1974. Characterization and immobilization of *Escherichia Coli* ATCC-26 β -galactosidase. *Biotechnol. Bioeng.* 16, 1633.
- WOYCHIK, J.H. and WONDOLOWSKI, M.V. 1972. Covalent bonding of fungal β -galactosidase to glass. *Biochem. Biophys. Acta.* 289, 347.
- WOYCHIK, J.H. and WONDOLOWSKI, M.V. 1973. Lactose hydrolysis in milk and milk products by bound fungal β -galactosidase. *J. Milk Food Technol.* 36, 31.
- WOYCHIK, J.H., WONDOLOWSKI, M.V. and DAHL, K.J. 1974. Preparation and application of immobilized β -galactosidase of *Saccharomyces lactis*. In *Immobilized Enzymes in Food and Microbial Processes.* (A.C. Olsen and C.L. Cooney, eds.) 41 pp. Plenum Press, New York.

ERROR ANALYSIS IN ESTIMATING THERMAL DIFFUSIVITY FROM HEAT PENETRATION DATA¹

JOHN W. LARKIN² and JAMES F. STEFFE³

Michigan State University
East Lansing, MI 48824

Received for Publication May 10, 1982

Accepted for Publication September 2, 1982

ABSTRACT

The ability to predict thermal diffusivity from heat penetration data containing normally distributed errors in can dimensions, measurements in time, measurements of temperature, thermocouple probe location, and assumptions concerning surface heat transfer coefficients was investigated using a nonlinear least squares solution of Fourier's heat conduction equation. Thermal diffusivity calculated from heat penetration data is largely dependent on errors associated with temperature measurement and to a lesser extent dependent on errors in thermocouple probe location. Errors in can dimensions and time measurement had only a minor influence on the prediction of thermal diffusivity. Best prediction accuracy is obtained under the following conditions: (1) When a large can with a length over diameter ratio close to 0.8 is used; (2) when the difference between the initial and heating medium temperature is greater than 40°C; (3) when the data used for calculation of thermal diffusivity is limited to the temperature ratio range of 0.15 to 0.85; (4) when the Biot Numbers for the surfaces of the can are measured or known to be greater than 200; (5) when an accurate time clock is used, and when the position of the thermocouple probe is accurately known.

INTRODUCTION

In recent years numerous thermal prediction models (Lenz 1977; Teixeira *et al.* 1969; Ohlsson 1980) have required an accurate value of thermal diffusivity (α) to be known. A recent review by Singh (1981) describes a number of different methods used in determining thermal diffusivity. Thermal diffusivity values have been approximated mostly

¹ Michigan Agricultural Experiment Station
Journal Article Number 10496

² Department of Food Science and Human Nutrition

³ Department of Agricultural Engineering

by first term approximation (Gaffney *et al.* 1980) or because of the proliferation of thermal process data, from their relation to f_h as proposed by Olson and Jackson (1942). For the most part authors (Ohlsson 1980; Hicks 1961; Teixeira *et al.* 1969) have adopted Olson and Jackson's (1942) equation for estimating α .

Since Olson and Jackson's (1942) publication a number of incongruities have been pointed out, the first being the lack of agreement in calculated (α) from heat penetration tests using different size cans (Teixeira *et al.* 1975). The second one is the potential error in α associated with neglecting the surface heat transfer coefficients (Uno and Hayakawa 1980; Bhowmik and Hayakawa 1979; Gaffney *et al.* 1980) and the last one is that lack of a sufficient number of terms in the infinite series solution to Fourier's heat conduction equation (i.e., first term approximation error; Lenz 1977; Albin *et al.* 1979).

Teixeira *et al.* (1975) attributed the lack of agreement in α values for different can sizes to heat penetration down the thermocouple leads, resulting in a larger α value for the smaller cans. Ecklund (1956) investigated heat penetration effects in a number of can sizes, where it was pointed out that if a thermocouple is mounted such that its receptacle projects into the can, as in nonprojecting plug-in thermocouples (Ecklund 1949), the rate of heating increases significantly, but the f_h values do not change. In addition, it was stated that the size of the thermocouple wires used in the analysis did not contribute appreciably to any error. Thus the error (change in j_h values) in heat penetration data is almost entirely due to the receptacle of the nonprojecting plug-in type thermocouples, not due to the leads of the thermocouple. Therefore, since heat conduction down the thermocouple leads does not appreciably affect the f_h values, some other factor must cause the discrepancy in calculated α values for different can sizes.

Uno and Hayakawa (1980a) and Bhowmik and Hayakawa (1979) point out that neglecting surface heat transfer coefficients (h) may not be justified due to head-space and retort packing effects. To correct for this Bhowmik and Hayakawa (1979) developed a method where a long cylinder is used to estimate both α and h values. Bhowmik and Hayakawa (1979) did this by solving (using first term approximation) the analytical solution of heat penetration in an infinite cylinder with a finite surface heat transfer coefficient. Then from a heat penetration test they calculated α and h . Uno and Hayakawa (1980a) however, developed a procedure where α and h_i where $i = t, b, s$ (h is finite and different on each side of a can; h_t = surface heat transfer coefficient for the top, h_b = surface heat transfer coefficient on the bottom, and h_s = surface heat transfer coefficient for the side) can be estimated from actual heat penetration data from a can. No special equipment is

needed for this method, but four thermocouples must be used which could lead to errors such as those described by Ecklund (1956). In an error analysis of this latter method, errors of 1 mm in location and dimensional quantities, 1°C in temperature, and 5% in f_h , values were used to predict a maximum relative error value of 24.6% for α in a 300 × 409 can. An error of this magnitude tends to make this method of estimation undesirable even though the factors used to calculate the error were not unreasonable.

Instead of using a first term approximation method Lenz (1977) used the infinite series solution to Fourier's heat conduction equation adding terms until no appreciable difference occurred between successive totals. Lenz (1977) solved for α by using a modified Newton-Raphson method (this was described as a least squares procedure, which might be more appropriately called a nonlinear least squares procedure). Albin *et al.* (1975) also used a nonlinear least squares procedure to calculate δ but the exact numerical procedure was not indicated.

Hayakawa and Bakal (1973) used a nonlinear least squares procedure to calculate δ in a finite slab when there was a known changing surface temperature. All of Hayakawa and Bakal's (1973) results were with regards to freezing and thawing foods. The nonlinear least squares procedure allows for the solution of more than one independent variable at a time. Thus, heat penetration data can be used to calculate α as well as h_i where $i = t, b, s$. In addition to calculating the independent parameters an approximation of their standard deviations can be made. Lenz (1977) and Albin *et al.* (1975) neglected h values and only calculated α .

A nonlinear least squares procedure is a superior method to use in estimating α and h_i values from heat penetration data because the potential errors of assuming infinite surface heat transfer coefficients and using first term approximations of the infinite series solution of Fourier's heat conduction equation can be eliminated. Before this model can be fully advocated an investigation of the analytical solution to Fourier's heat conduction equation must be made. The investigation was limited to material factors (i.e., not biological factors). Initially, these factors were identified as: (1) can size variations; (2) geometric misalignment of the thermocouple; (3) measurements of time; (4) measurements of temperature; (5) heat penetration down the thermocouple probe and; (6) having finite surface heat transfer coefficients, but assuming infinite values. From Ecklund's (1956) results the authors assumed that all heat penetration tests were done with thermocouples mounted on the surface of the can (i.e., not recessed) allowing us to neglect the error related to heat penetration down the thermocouple probe. After the above factors are investigated the infinite series

solution of Fourier's heat conduction equation will be investigated by calculating errors associated with first term approximations of f_h values. Associated α values will be calculated from Olson and Jackson's (1942) equation, and comparisons between this α value and nonlinear least squares values of α will be made.

When α was estimated by Teixeira *et al.* (1975) using first term approximations the most accurate value of α was assumed to be that for the 603×700 can, because it had a j_h value close to the theoretical value (this j_h value was probably in error due to the nonprojecting thermocouples (Ecklund 1956)). A difference in α of 15.2% was seen by Teixeira *et al.* (1975) for the 303×406 and 603×700 cans.

THEORETICAL DEVELOPMENT

The following were assumed for all models used in this analysis: (1) physical and thermal properties of the food products are not temperature dependent; (2) products are homogeneous, isotropic materials; (3) the food is heated by conduction (i.e., it follows Fourier's equation of heat conduction); (4) the product has a uniform initial temperature; (5) environmental changes are instantaneous (i.e., no lag time in retort come-up); (6) surface resistance will consist of apparent h values associated with external surface convection, conduction in container material and internal surface convection and; (7) there is no phase change in the product during heating. In conjunction with these assumptions only the heating phase will be analyzed.

Fourier's equation of heat conduction with no internal heat source for an infinite slab is

$$\frac{\partial^2 TR}{\partial x^2} = \frac{1}{\alpha} \frac{\partial TR}{\partial \theta} \quad (1)$$

The analytical solution (Özişik 1980) to Eq. (1) for a thickness of $2L$, a surface heat transfer coefficient of h for the top and bottom of the slab, and origin at the center is

$$TR = \frac{T - T_m}{T_i - T_m} = 2 \sum_{n=1}^{\infty} \left[\frac{\sin(\lambda_n)}{\lambda_n + \sin(\lambda_n) \cos(\lambda_n)} \right] \exp \left[\frac{-\lambda_n^2 \alpha \theta}{L^2} \right] \cos(\lambda_n \frac{\alpha}{L}) \quad (2)$$

with

$$\begin{aligned} \lambda_n &= \text{roots of } \lambda_n \tan \lambda_n = \text{Bi} \\ \text{Bi} &= \text{Biot number for the slab} = hL/K \end{aligned}$$

- α = thermal diffusivity
 x = distance from center
 T_m = temperature of heating medium
 T_i = uniform initial temperature of the slab, i.e., temperature at $\theta = 0.0$
 θ = time
 T = temperature in the slab at time θ and point x

satisfying the following initial and boundary conditions:

$$\begin{aligned}
 TR &= 1.0 \text{ when } \theta = 0.0 \\
 \frac{\partial TR}{\partial x} &= 0 \text{ when } x = 0.0 \\
 \frac{\partial TR}{\partial x} &= \frac{-h}{k} TR \text{ when } x = L
 \end{aligned}$$

When h is assumed infinite, $TR = 0$ at $x = L$, then Eq. (2) reduces to

$$TR = \frac{4}{\pi} \sum_{n=1}^{\infty} \frac{(-1)^{n+1}}{(2n-1)} \cos\left(\frac{(2n-1)\pi x}{2L}\right) \exp\left[-\left(\frac{(2n-1)\pi}{2}\right)^2 \frac{\alpha\theta}{L^2}\right] \quad (3)$$

Fourier's equation for heat conduction for an infinite cylinder with no internal heat source is

$$\frac{1}{r} \frac{\partial TR}{\partial r} + \frac{\partial^2 TR}{\partial r^2} = \frac{1}{\alpha} \frac{\partial TR}{\partial \theta} \quad (4)$$

The analytical solution (Özişik 1980) to Eq. (4) for a cylinder of radius R , having a surface heat transfer coefficient of h , origin along the cylindrical axis is

$$TR = 2 \sum_{n=1}^{\infty} \frac{1}{\beta_n} \frac{J_1(\beta_n) J_0(\beta_n \frac{r}{R})}{J_0^2(\beta_n) + J_1^2(\beta_n)} \exp\left[\frac{-\beta_n^2 \alpha \theta}{R^2}\right] \quad (5)$$

with

- β_n = roots of $\beta_n J_1(\beta_n) = (\text{Bi}) J_0(\beta_n)$
 J_0 = Bessel Function of the first kind, of order zero
 J_1 = Bessel Function of the first kind, of order one
 r = distance from the center
 Bi = hR/k

satisfying the following initial and boundary conditions:

$$\begin{aligned} TR &= 1.0 \text{ when } \theta = 0.0 \\ \frac{\partial TR}{\partial r} &= -\frac{h}{k} TR \text{ at } r = R \\ \frac{\partial TR}{\partial r} &= 0 \text{ at } r = 0.0 \end{aligned}$$

When h is assumed infinite, $TR = 0$ at $r = R$, then Eq. (5) reduces to

$$TR = 2 \sum_{n=1}^{\infty} \frac{J_0(\beta_n \frac{r}{R})}{\beta_n J_1(\beta_n)} \exp\left[-\frac{\beta_n^2 \alpha \theta}{R^2}\right] \quad (6)$$

where β_n are the roots of $J_0(\beta_n) = 0$

The analytical solution (Uno and Hayakawa 1979; Özişik 1980) to Eq. (1) for a slab thickness of $2L$, surface heat transfer coefficient for the top and bottom of h_t and h_b respectively, and origin at the bottom of the slab is

$$\begin{aligned} TR &= 2 \sum_{n=1}^{\infty} \exp\left[-\frac{\gamma_n^2 \alpha \theta}{4L^2}\right] \frac{(\gamma_n^2 + \text{Bi}_t^2)(\gamma_n \cos(\gamma_n x) + \text{Bi}_b \sin(\gamma_n x))}{(\gamma_n^2 + \text{Bi}_b^2 + \text{Bi}_b)(\gamma_n^2 + \text{Bi}_t^2) + \text{Bi}_t(\gamma_n^2 + \text{Bi}_b^2)} \\ &\quad \left[\sin(\gamma_n) + \frac{\text{Bi}_b(1 - \cos(\gamma_n))}{\gamma_n} \right] \end{aligned} \quad (7)$$

with

$$\begin{aligned} \gamma_n &= \text{roots of } \tan(\gamma_n) = \frac{(\text{Bi}_b + \text{Bi}_t)\gamma_n}{\gamma_n^2 - (\text{Bi}_b \text{Bi}_t)} \\ \text{Bi}_t &= \text{Biot number for top of slab, } = h_t 2L/k \\ \text{Bi}_b &= \text{Biot number for bottom of slab, } = h_b 2L/k \\ x &= \text{distance from bottom of slab.} \end{aligned}$$

satisfying the following initial and boundary condition:

$$\begin{aligned} TR &= 1.0 \text{ when } \theta = 0.0 \\ \frac{\partial TR}{\partial x} &= \frac{h_b}{k} TR \text{ at } x = 0 \\ \frac{\partial TR}{\partial x} &= -\frac{h_t}{k} TR \text{ at } x = 2L \end{aligned}$$

The product of Eq. (5) or (6) and (2), (3), or (7) represent the heat transfer model used during this study. Equation combinations were selected depending on whether or not there was symmetric or nonsymmetric heating for the top and bottom of the can and/or if the surface heat transfer coefficient was assumed infinite because less computer time was required for calculation of (6) than (5) and less time was required for the calculation of (3) than (2) or (7). Each of the above equations were written as FORTRAN-77 subroutines which could be used by any of the programs developed during the study.

ANALYTICAL PROCEDURE

Five can sizes (307×409, 307×306, 307×512, 202×308 and, 603×700) were selected for this investigation (Table 1). The first three can sizes were chosen for their constant radius, moderate size and, varying L/R ratios. Can sizes 202×308 and 603×700 were chosen to represent small and large cans often used in industry.

The variables used for the error analysis of the model consisted of: time (θ), temperature (T), length dimension of the can size ($2L$), radius dimension of the can size (R), radial location of the thermocouple probe (r), and axial location of the thermocouple (x), and surface heat transfer coefficients (h_i , where $i = t, b, s$). The surface heat transfer coefficient is not as much an error in measurement as it is in the assumptions drawn by the experimenter; i.e., most calculations assume h is infinite and uniform along the can which is often incorrect. This is an error which one can account for knowingly; therefore, errors associated with the assumption of h were analyzed after the other factors were investigated.

With the advent of microelectronics numerous data acquisition units have been produced that allow for very accurate and precise temperature and time measurements. In addition to the data-acquisition unit's

Table 1. Can size used in generating data

Can Number	Radius (R) (m)	Half Height (L) (m)	L/R
307 × 409	.04366	.05794	1.327
307 × 306	.04366	.04286	.9818
307 × 512	.04366	.07303	1.673
202 × 308	.02699	.04445	1.647
603 × 700	.07858	.0889	1.131

increased precision they also eliminate the human error associated with reading data off a chart-type recorder. Therefore, the authors assumed that errors associated with time and temperature measurements were not a result of human variations but due solely to mechanical variations. Time variations (95% confidence interval) used in this study followed an autoregressive order with an error in time of $\pm 0.005\%$ (θ) ± 1 s which is the case for a typical data acquisition system such as the Hewlett Packard Model 3054DL. For the temperature factor, copper-constantan thermocouples were assumed which, in the range of interest (20-130°C), produced a measurement error of the order of ± 0.5 to 1.0°C . In this study, the errors for probe locations were made the same for each can and set so that a 95% confidence interval of error related to ± 4.0 mm for the radial placement and ± 4.0 mm for the axial placement. Due to the high precision needed to ensure proper lid closure and seam formation, this work assured two thousandths of an inch variations in can length and diameter, which results in a 95% confidence region of error equal to ± 0.5 mm for can length and diameter. Surface Biot Number variations were assumed to range from 10 to ∞ . A summary of errors (for a 95% confidence region) used in the measurement of the model conditions is listed in Table 2. Populations of normally distributed points were generated using the Box-Muller transformations on a set of pseudorandom numbers (Beck and Arnold 1977). These points were then transformed using the mean and standard deviations of the specific parameter(s) under investigation to obtain normally distributed points from which the heat transfer model could be tested.

To analyze the error factors a set of calculated or "actual" data points were produced with $\alpha = .00062 \text{ m}^2/\text{h}$, $h \rightarrow \infty$, the thermocouple probe located at the center, and no errors in time or temperature or can

Table 2. Error factors used to generate data to analyze the analytical solution to Fourier's heat conduction equation

Factor	Attribute Standard Deviation
Time	.000025 $\theta \pm 1$ sec
Temperature	.33333 $^\circ\text{C}$
Can half length	.000125 m
Can radius	.000125 m
Probe location (axially)	.002 m
Probe location (radially)	.002 m
	Range
Surface biot numbers (Bi_t , Bi_b , and Bi_s)	10.0 to ∞

dimensions. From each "actual" time data point used, a set of 150 points were generated with an assumed error factor. For each point generated a α value was calculated using a direct search method (Beck and Arnold 1977) such that $(T_a - T_c)^2$ was minimized, with T_a equal to the actual temperature and T_c equal to the calculated temperature (T_i was always equal to 62.0°C and T_m was always equal to 121.1°C).

The mean and standard deviation was recorded for each set of 150 α values, with the standard deviation measured about the "actual" value of α (.00062 m²/h). Each parameter (except Bi) listed in Table 2 was varied individually to test its effect on the heat transfer model, then all the parameters (except Bi) in Table 2 were varied at the same time.

From the combined effect of all the error factors (except Bi) of Table 2 a distribution of the mean and standard deviation of α was obtained with respect to temperature. From this error distribution a population of 20 temperature values was created for each known mean and standard deviation (50 values) of α , for nine different values of Bi (ranging from 10 to ∞). This gave a total of 1000 points for each Bi number for a total of 9000 points. Thermal diffusivity values were calculated assuming an infinite h value such that $\sum_{i=1}^{1000} (T_{a,i} - T_{c,i})^2$, using nonlinear least squares (Móre *et al.* 1981), was minimized. Recall that T_a refers to points produced assuming $\alpha = .00062$ m²/h and Bi is a value in the range specified in Table 2.

The same populations of data points discussed above were used to simulate a heat penetration test from which f_h values were calculated. Calculation of f_h values were carried out with a FORTRAN-77 subroutine which maximized the coefficient of determination (r^2) of the data by regressing the data for a specific number of points and then regressing the data again with one less point (removing the smallest time value). The elimination of points was repeated until the data with one less point had a coefficient of determination lower than the one with one more point.

RESULTS AND DISCUSSION

Two statistics that are usually used to describe the distribution of populations are the mean (μ) and standard deviation (σ). For ease of comparisons, the results of error analysis are described by the residuals of the mean ($\epsilon = (\mu - \bar{x})$; where \bar{x} = estimate of μ) and the coefficient of variance ($C_v = s/\mu \times 100$; where s = estimate of σ). Plots of ϵ/μ and C_v versus TR for each of the error factors (Table 2) and a plot of the composite effect of all the error factors are depicted in Fig. 1 through 10. When viewing Fig. 1 through 10 it should be realized that TR varies

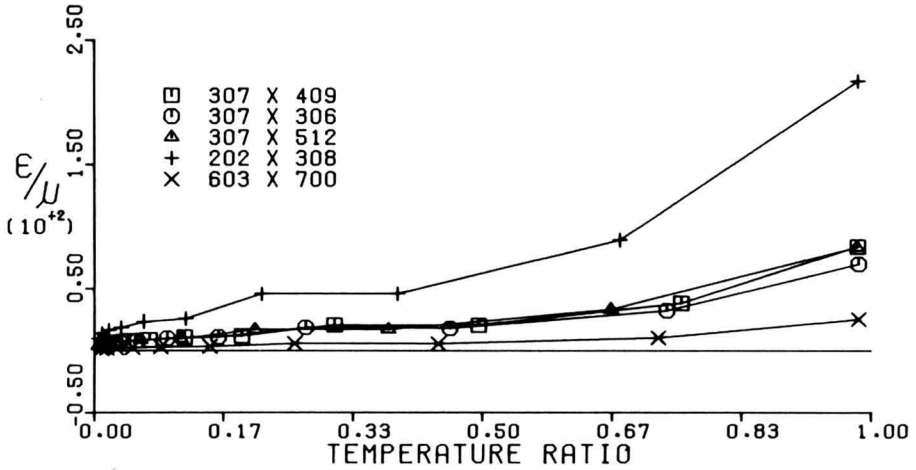


FIG. 1. RESIDUAL ERROR DISTRIBUTION FOR ERROR IN RADIAL PLACEMENT OF THE THERMOCOUPLE PROBE

from one to zero with complete heating. From Fig. 1, 3, and 5 it can be seen that variations in thermocouple probe location, can dimension, and time result in low ϵ values for long time periods.

Errors in thermocouple probe location result in ϵ values that are all positive (Fig. 1 and 3) because the thermocouple probe was located at the slowest heating point of the can. Hence, an error in thermocouple

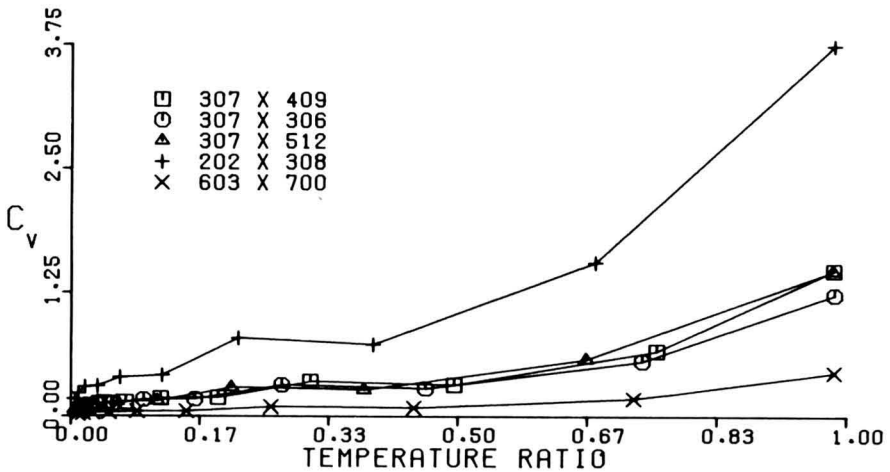


FIG. 2. VARIANCE DISTRIBUTION FOR ERROR IN RADIAL PLACEMENT OF THE THERMOCOUPLE PROBE

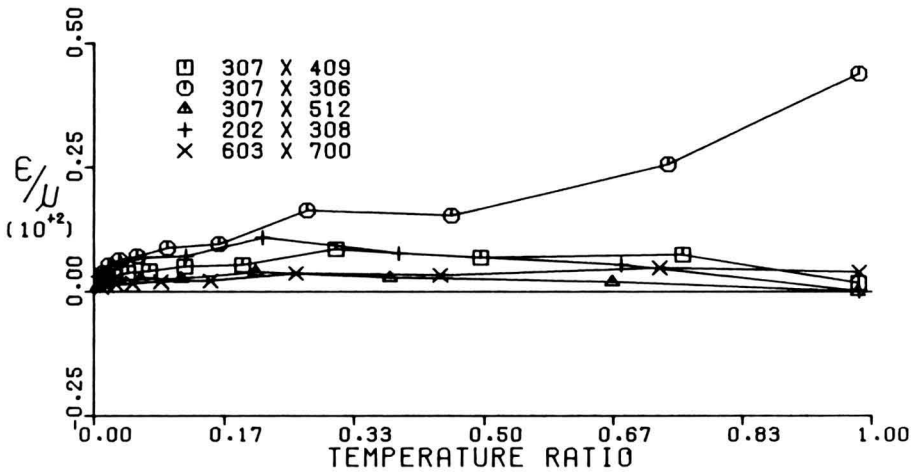


FIG. 3. RESIDUAL ERROR DISTRIBUTION FOR ERROR IN AXIAL PLACEMENT OF THE THERMOCOUPLE PROBE

probe location will always result in an underestimation of the actual values of α . The underestimation of α for an error in probe location is the largest for the can with the largest relative heat penetration rate and the smallest dimensions. What this means is that there are two factors influencing the error associated with probe location. The first is the level of the heat penetration rate for one dimension as compared with that of the other dimension (L/R). The second is the relative misplacement of the thermocouple probe with respect to the length of the dimension of misplacement. For example, in the case of the 202×308 can the majority of the heat penetration is from the radial direction (i.e., a large L/R , Table 1). In addition, the 202×308 has a small radius, where the same displacement in thermocouple probe (in all the cans studied) results in a larger relative displacement from the center. Thus, as seen in Fig. 1, the 202×308 can has the largest ϵ values for any can associated with error in the radial placement of the thermocouple probe.

The magnitude of ϵ (Fig. 1 and 3) is a result of the fact that shortly after the cans start to heat a gradient in temperature near the center is established for both the radial and axial directions. For the 202×308 can the radial gradient in temperature in the center is greater than the other cans due to a large L/R and small radius. As the can is heated the temperature gradient around the center and the ϵ values associated with the thermocouple probe location decrease. The axial effect for the 202×308 can (Fig. 3) is very different, because with high TR values the

error in axial probe placement is negligible. This indicates that initially there is virtually no temperature gradient near the can center in the axial direction. As the heating of the can continues a larger gradient is established and with it larger ϵ value. The ϵ values increase for the axial direction until the temperature gradient near the center starts to decrease with time, after which the ϵ values decrease with continued heating. Figure 3 also shows that as the L/R ratio decreases (Table 1) the axial heat penetration rate grows in prominence, resulting in larger ϵ values for low time (see, for example, the 307×306 can). The 603×700 ($L/R = 1.13$) can seems to be near a transition point (Fig. 3) where the prominence of the axial heat penetration rate is felt. The underestimation of α that occurs from errors in thermocouple probe location have associated with it a changing magnitude of precision (C_v) (Fig. 2 and 4). Precision in the radial direction for the 202×308 can reached a C_v of 4.0% for low time where the C_v for the 603×700 can never exceeded 0.5%. The axial C_v values generally remain low for all can sizes, the 603×700 being the lowest with the C_v value having a maximum of approximately 0.1%. This indicates that the error in estimating α values due to an error in thermocouple probe location will be minimized by minimizing the relative error of the thermocouple probe location. In addition, the L/R value of the can should be such that the heat penetration rates for both axial and radial directions are nearly equal. This can be accomplished using L/R value in the range of .70 to .80.

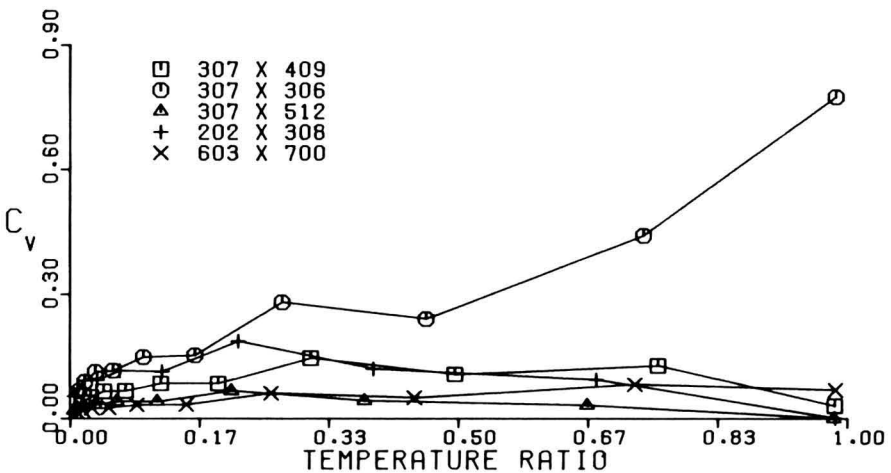


FIG. 4. VARIANCE DISTRIBUTION FOR ERROR IN AXIAL PLACEMENT OF THE THERMOCOUPLE PROBE

The effect of variations in actual can size on estimating α values were found to be smaller than the effect from variations in thermocouple probe location. This is because the magnitude of can size errors are much smaller than probe position errors. Can size variations gave ϵ values approximately ten times less and C_v values approximately four times less than those found with variations in probe location. Due to the small magnitude of ϵ and almost constant C_v values for the TR range, the actual effect of can size variations on calculation of α are miniscule and may be ignored.

Time variations result in error effects (Fig. 5 and 6) very similar to the error effects of can size, both in magnitude and trend. However, there are decreasing C_v values for decreasing TR values where there was no trend in C_v for the can size factor. The ϵ values are the largest for the cans with the fastest heating rate. Indicating that a can that heats slowly will result in a more accurate α value even though the error in time increases with longer time periods. The high accuracy of the clock used during this study resulted in small values of ϵ and C_v which in turn do not cause any real appreciable changes on the calculation of α and thus any error in time measurement may be ignored.

Temperature variations resulted in the largest errors for any one error factor investigated (Fig. 7 and 8). This means temperature is the most significant parameter in controlling the accuracy of the α estimation. This significance is not only due to the magnitude of C_v and ϵ but

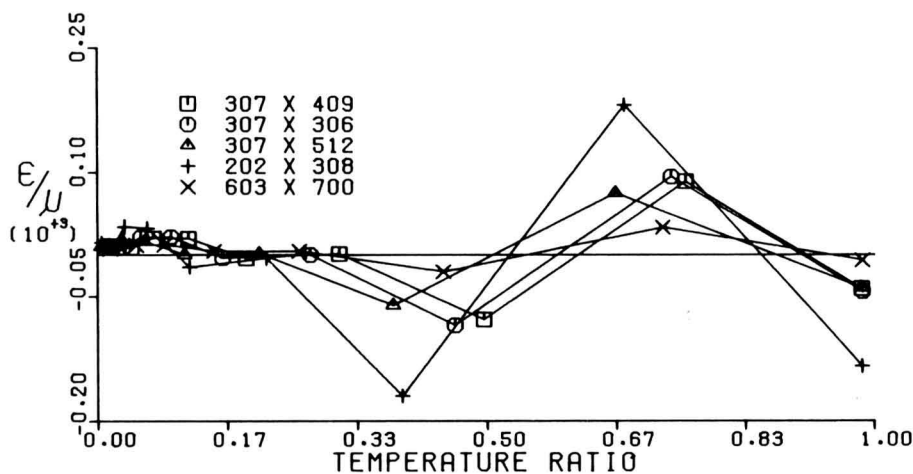


FIG. 5. RESIDUAL ERROR DISTRIBUTION FOR THE AUTOREGRESSIVE ERROR IN THE MEASUREMENT OF TIME

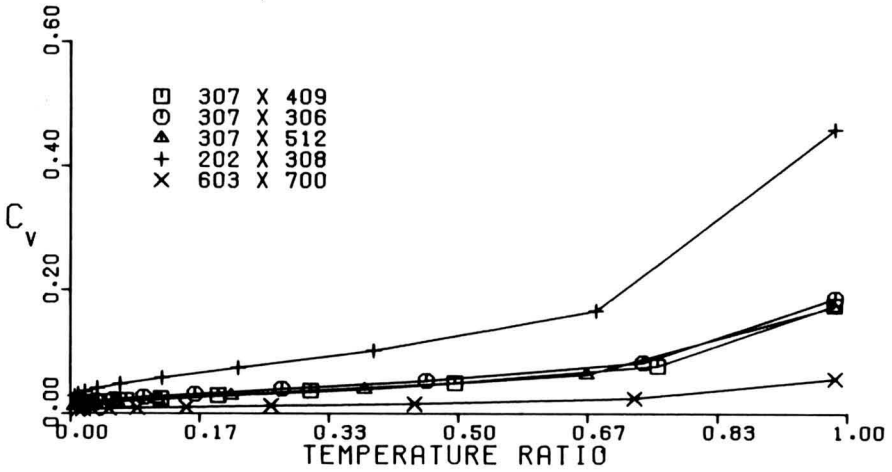


FIG. 6. VARIANCE DISTRIBUTION FOR THE AUTOREGRESSIVE ERROR IN MEASUREMENT OF TIME

also due to the trends the ϵ and C_v values display in relation to TR . The shapes are significant because the curves are identical for the different can sizes (as might be expected from observations of transient heat conduction charts) and because they show a violation of a well-accepted assumption for high and low TR ranges, i.e., that the errors in temperature measurement do not bias the calculation of α . Fig. 7

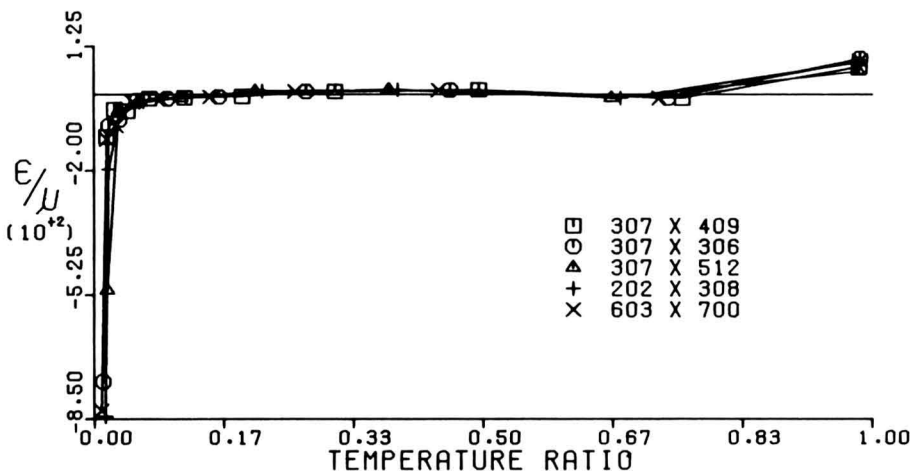


FIG. 7. RESIDUAL ERROR DISTRIBUTION FOR THE ERROR IN THE MEASUREMENT OF TEMPERATURE

indicates that the assumption of unbiased α values can only be accepted in the TR range of approximately .90 to .05. Outside the range α values are biased upward for low TR and downward for high TR values. Another important point is that an α value calculated strictly with low or high values of TR will not only be inaccurate but also be less precise due to the increasing values of C_v outside the TR range of 0.85 to 0.15. (Fig. 8)

The influence of temperature on the calculation of α predominates when all the factors listed in Table 2 (except for Bi) are varied at once (Fig. 9 and 10). When Fig. 9 and 7 are compared a drifting upward of ϵ values is noticed for increased TR when all the error factors are varied. This was not present when only temperature was varied. The upward trend in ϵ values for Fig. 9 is just like that observed for the ϵ values associated with error in thermocouple probe location (Fig. 1 and 3). In this study the more important error in thermocouple probe location is the radial displacement error because all the cans considered have L/R values above 0.8. Therefore, for the sizes and ranges of error factors considered, the predominant error factors in the calculation of α are temperature measurement and radial placement of the thermocouple probe. When only the measurement in temperature was an error factor a TR range of .85 to .15 was specified from which an accurate and precise value of α could be calculated; however, with the addition of the thermocouple probe location error a tighter upper bound on TR might be in order for cans having L/R values different from 0.8.

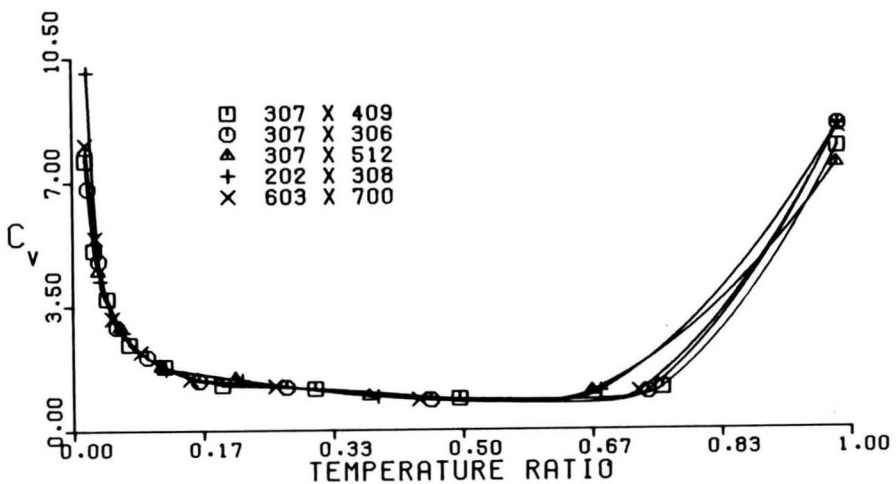


FIG. 8. VARIANCE DISTRIBUTION FOR THE ERROR IN THE MEASUREMENT OF TEMPERATURE

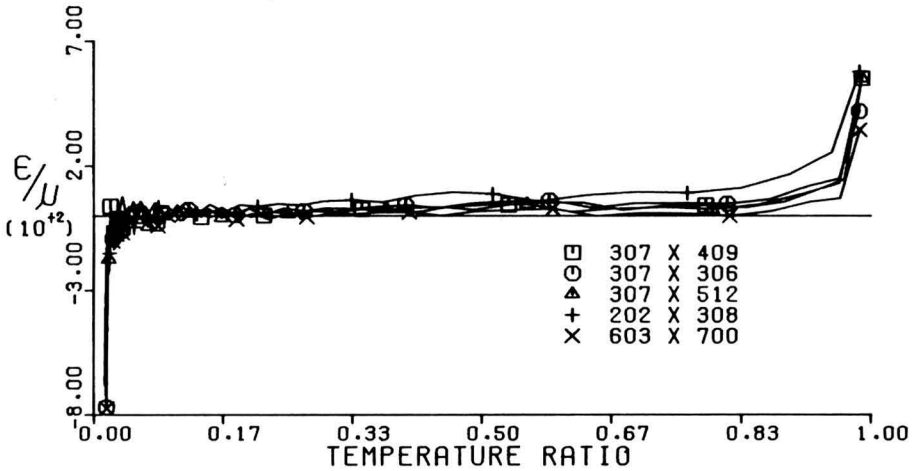


FIG. 9. RESIDUAL ERROR DISTRIBUTION FOR THE COMBINATION OF THE ERROR FACTORS INVESTIGATED

When the temperature difference (ΔT) between the initial product temperature and the medium temperature was varied from 121.1°C to 11.1°C (previously held constant at 56.1°C) the shape of the residual error (ϵ) and coefficient of variance (C_v) curves remained the same as found in Fig. 9 and 10 discussed above. There was however, a noticeable

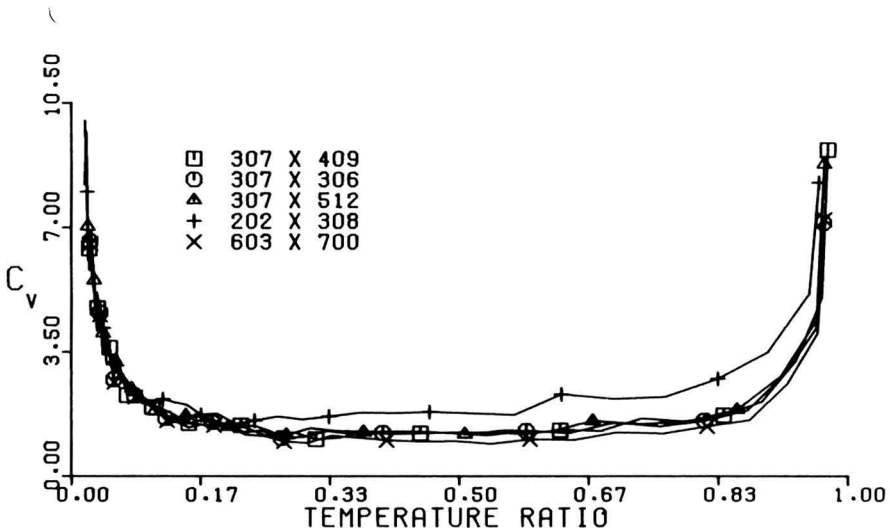


FIG. 10. VARIANCE DISTRIBUTION FOR THE COMBINATION OF THE ERROR FACTORS INVESTIGATED

difference in the level of the constant C_v region (TR range of .15 to .85). A coefficient of determination of .9987 was obtained when the mean value of C_v , for the TR range of .15 to .85, was fitted against the inverse of ΔT as

$$C_v = .2677 + \frac{62.21}{\Delta T} \tag{8}$$

Equation 8 shows that the precision (C_v) associated with estimating α decreases drastically as ΔT decreases below 40.0°C; thus, to obtain an accurate estimate of α the ΔT should remain above 40.0°C.

From the distribution of α in Fig. 9 and 10 additional populations of time-temperature points were generated with varying Bi values ($Bi_t = Bi_s = Bi_b$), and compared with time-temperature data calculated assuming $1/Bi = 0.0$ (Fig. 11). Due to the complexity of trying to analyze the effect of different and varying Bi values for the top, bottom and side of a can the Biot Number values were assumed to be the same for all the surfaces of the can. This assumption was made because the error associated with Bi values is one of assumption (the researcher assumes it is a specific value), or of a previous measurement. When the researcher does not know if the Biot Numbers are significant in calculating α , the product of Eq. 5 and 7 should be used as the model because this model allows for estimation of all four of the independent variables (α, Bi_b, Bi_t, Bi_s) using a nonlinear least squares procedure.

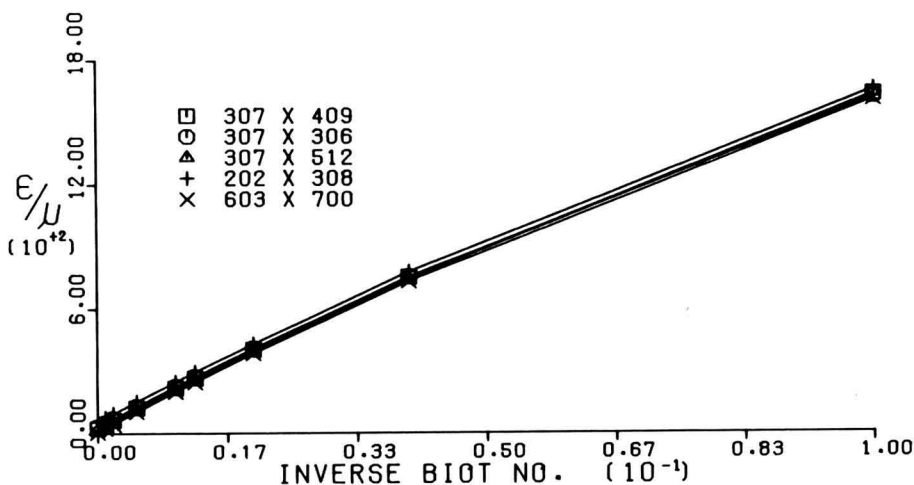


FIG. 11. RESIDUAL ERROR DISTRIBUTION FOR ERROR IN THE ASSUMPTION OF THE BIOT NUMBER USED IN PROCESSING

From Fig. 11 it can be seen that the calculation of α is biased downward when the actual Bi values are not equal to infinity. A 4.0% bias occurs when Bi is actually equal to 50, which indicates that even though current literature gives different values for critical Bi numbers to describe the transition zone for an insignificant surface effect (usually, $Bi > 40$), a 4.0 to 4.5% error in the calculation of α can be made by neglecting such effects. Similar results as these were obtained by Gaffney *et al.* (1980) for a first order approximation model. The accuracy in the determination of α values starts to deviate as soon as the Bi values migrate from infinity and the standard deviation of α does not significantly start to increase (for errors in assumptions in Bi) until Bi is less than 25. In addition, increases in the standard deviation are practically independent of can size.

From the same population of time-temperature points, with varying Bi values a similar potential error of 4.0% in α can be obtained in the calculation of α from f_h . This occurs using the Olson and Jackson (1942) Eq. (9), where Bi was equal to 50 but was assumed infinite. The equation may be written as

$$f_h = \left(\frac{1}{\alpha}\right) \frac{.398}{\left(\frac{1}{R^2} + \frac{.4267}{L^2}\right)} \quad (9)$$

The α value calculated from the analytical model always resulted in an underestimation of α whereas the Olson and Jackson equation first overestimated the actual α value and then underestimated α as the Bi values decreased. In Fig. 9 it can be seen that the α values start to be biased upward as the TR values decrease. This causes the α value calculated from Olson and Jackson's equation to be overestimated, since the slope of the heating curve is increased due to the increasing upward bias of α and because the calculation of f_h is more dependent on the lower TR values. Calculation of α from the analytical model places more importance on the intermediate values of TR where, due to the error in thermocouple probe location, the α values are biased downward resulting in an underestimation of α .

The overestimation of α from f_h for the different can sizes ($Bi = \infty$, is data set 1) does not follow the same trend as that for the underestimation of α for the analytical model (Table 3). The value of α calculated from the analytical model for the 603×700 can was very accurate and a similar accuracy was expected for the α value calculated from the f_h values. In turn the 307×409 can gave the most accurate value of α calculated from f_h , with the value of α from f_h for the 603×700 can having a lower accuracy. To determine if this type of trend was due to

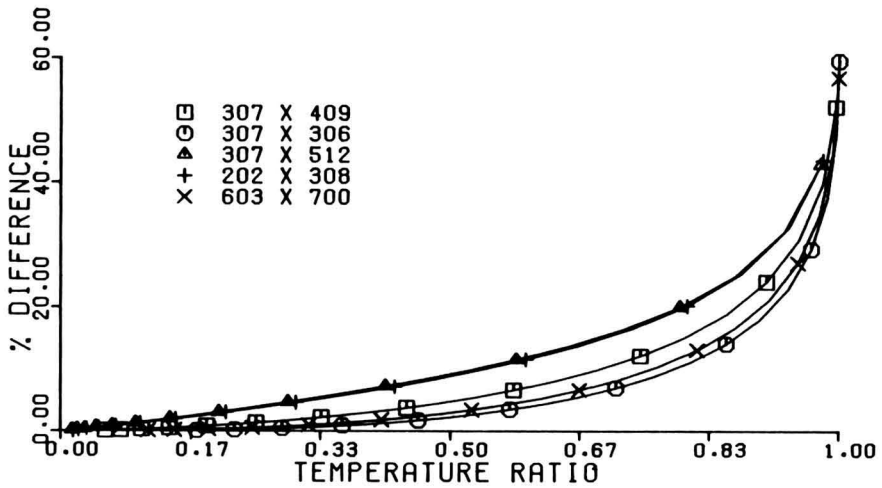


FIG. 12. PERCENT DIFFERENCE OF THE TEMPERATURE RATIO FOR THE FIRST TERM APPROXIMATION AND INFINITE SERIES SOLUTION

the errors associated with the data or first term approximation, a population of 100 points with a constant C_v (1.0%) for α , was generated and called data set 2. The f_h and α were calculated for each can size (Table 3) from this population of points. The same trend in can size was noticed in both the α values calculated from f_h for data set 1 and data set 2 (Table 3). From the similarity in trends of the two calculated α values it appears that the effect of the error terms in Table 2 on α is one of a linear (upward bias) shift in α and that the variation in error associated with the specific can dimensions is mostly due to the first term approximation method.

Table 3. Summary of α and f_h values obtained from different data sets (1-error distribution, 2-constant C_v of $\alpha = 1.0\%$)

Can Size	α	α from f_h	α from f_h
	Data Set 1	Data Set 1	Data Set 2
	α_1	α_2	α_3
	($m^2/h \times 10^{-3}$)	($m^2/h \times 10^{-3}$)	($m^2/h \times 10^{-3}$)
307 \times 409	.618	.621	.599
307 \times 306	.618	.627	.613
307 \times 512	.619	.624	.603
202 \times 308	.616	.624	.605
603 \times 700	.620	.625	.606

Actual $\alpha = .620 \times 10^{-3} m^2/h$

Figure 12 presents the first term approximation error ((approximation - actual) \times 100/(actual)), in the calculation of TR values for all five can sizes. As the L/R ratio increases, the error in the first term approximation increases. A L/R ratio of about .94 represents a can size where the error of first term approximation associated with the radial direction is the same as that in the axial direction. This explains why the 307 \times 306 can displays an α value closest to the actual value (Data Set 2, Table 3). This also explains why the error (except the 307 \times 409 can) in α calculated from f_h increases as the L/R increases. It is not known, without further investigation, why the 307 \times 409 can size deviates from the expected L/R ratio trend.

With the addition of the error factors listed in Table 2 the calculated α values from f_h become close to the actual α value. This is an apparent accuracy because it was assumed that heating follows Fourier's heat conduction equation; hence, the prediction of α calculated from f_h should follow the α values found using data set 2 instead of the apparently accurate α values calculated from data set 1. There is about a 3.5% change in the calculated α when the error factors in Table 2 are included in the calculations of α from f_h . If the errors in Table 1 change it becomes very difficult to make any judgement regarding how they will influence the estimation of α calculated from f_h because the estimated α values will fluctuate around the α values found from data set 2.

SUMMARY

A well-conditioned model is a model that performs as expected for a specific range of errors in the input parameters. With the original assumptions given at the beginning of this paper it was expected that the analytical solution to Fourier's heat conduction equation would yield a well-conditioned model to be used to accurately estimate the thermal parameters (α , and h_i ; where $i = t, s, b$) of a process. The condition of the analytical model was, when α was calculated from data ($h_i \rightarrow \infty$) containing errors (Table 2), largely dependent on the errors associated with temperature measurement and to a lesser extent dependent on errors in thermocouple probe location. Errors in can dimensions and time measurement had minor influence on the prediction of α , because of the magnitude of the error of the respective parameters. If there were only errors of can dimensions and time in a process they would indicate that a slowly heated can (large can) with a L/R ratio of about 0.8 should be used to increase the accuracy of the estimation of α . This same trend was noted for errors in thermocouple

probe location. Therefore, any actions taken to minimize the effect of error in thermocouple probe location would also minimize the effect of error occurring due to can dimensions and time measurement.

Can size was not a factor in influencing the condition of the model when only errors in temperature existed. For temperature errors the accuracy in predicting α ($h_i \rightarrow \infty$) was increased if the temperature data used was limited to a TR range of 0.85 and 0.15. This TR criteria predominates when all the error factors mentioned above are present. The thermocouple probe location error is also noticeable when all the errors (Table 2) are present, causing a tighter upper bound on the TR as the can size decreases and deviates from a L/R ratio of 0.8. In addition, when the Biot Number is assumed infinite but it is actually lower than 200 the model underestimates α by a value over 1.0%. This underestimation increases linearly with a decrease in the Biot Number.

When the first term approximation method was used in estimating α , large fluctuating α values ($h_i \rightarrow \infty$) resulted for different can sizes. The fluctuations occurred because of the reliance of Eq. (8) on the low, biased and highly variable, TR values. No procedures to increase the accuracy of α , when using the first term approximation method can be recommended without further analysis. However, when a nonlinear least squares method is used to estimate thermal parameters from Fourier's heat conduction equation, a number of procedures can be outlined to insure an accurate estimation of α .

CONCLUSIONS

The following guidelines should be followed when attempting to estimate the thermal parameters of Fourier's equation from heat penetration data, using the nonlinear least squares method:

1. Use as large a can as possible.
2. Use a can with a L/R ratio close to 0.8.
3. Measure, as accurately as possible, the position of the thermocouple probe after its placement and the inside dimensions of the can.
4. Use surface mounted thermocouple probes (or probes with the smallest amount of the mounting receptacle inside the can as possible).
5. To minimize errors in time measurement use an accurate data acquisition unit for data collection.
6. Calibrate the thermocouple probes to minimize errors in temperature measurement.

7. Allow for prediction of the surface heat transfer coefficients from the heat penetration data, or know and use the measured surface heat transfer coefficients in the estimation of α .
8. Limit range of data used in calculating thermal diffusivity to temperature ratio (TR) values between 0.15 and 0.85 (For errors consistent with those in Table 2).
9. The temperature difference between the initial product temperature and the heating medium temperature should not be lower than 40.0°C (For errors consistent with those in Table 2).

SYMBOLS

- Bi = Biot Number
 C_v = coefficient of variance (σ/μ)
 f_h = inverse slope of heat penetration curve (h)
 h = surface heat transfer coefficient ($W/m^2 \text{ } ^\circ C$)
 j_h = intercept for time zero of heat penetration curve
 J_0 = zero order Bessel Function of the first kind
 J_1 = first order Bessel Function of the first kind
 k = thermal conductivity ($W/m \text{ } ^\circ C$)
 L = half height of can or half thickness of an infinite slab (m)
 r = radial position in can (m)
 R = radius of can or radius of an infinite cylinder (m)
 s = estimate of standard deviation
 T = temperature ($^\circ C$)
 TR = temperature ratio = $(T - T_m)/(T_i - T_m)$
 x = axial position in can (m)
 \bar{x} = estimate of mean (m)

Subscripts

- a = actual
 b = bottom of can
 c = calculated
 i = initial or index number
 m = medium
 n = index number
 s = side of can
 t = top of can

Greek and Other

- α = thermal diffusivity (m^2/h)
 β = roots of eigenfunction for cylinder
 γ = roots of eigenfunction for nonsymmetrically heated slab

- θ = time (h)
 λ = roots of eigenfunction for symmetrically heated slab
 μ = mean of population
 π = the constant 3.14156
 σ = standard deviation of population
 ϵ = residual of mean ($\mu - \bar{x}$)
 ∞ = infinity

REFERENCES

- ALBIN, F.W., BADARI NARAYANA, K., SRINIVASA MURTHY, S. and DRISHNA MURTHY, M.V. 1979. Thermal diffusivity of some unfrozen and frozen food models. *J. Food Technol.* 14, 361-367.
- BECK, J.V. and ARNOLD, K.J. 1977. *Parameter estimation in Engineering and Science*. Chapter 4. John Wiley & Sons, New York.
- BHOWMIK, S.R. and HAYAKAWA, K. 1979. A new method for determining the apparent thermal diffusivity of thermally conductive foods. *J. Food Sci.* 44, 469-474.
- ECKLUND, O.F. 1949. Apparatus for the measurement of the rate of heat penetration in canned foods. *Food Technol.* 3, 231-233.
- ECKLUND, O.F. 1956. Correction factors for heat penetration thermocouples. *Food Technol.* 10, 43-44.
- GAFFNEY, J.J., BAIRD, C.D. and ESHLEMAN, W.D. 1980. Review and analysis of the transient method for determining thermal diffusivity of fruits and vegetables. *ASHRAE Transactions.* 86, 261-280.
- HAYAKAWA, K. and BAKAL, A. 1973. New computational procedure for determining the apparent thermal diffusivity of a solid body approximated with an infinite slab. *J. Food Sci.* 38, 623-629.
- HICKS, E.W. 1961. Uncertainties in canning process calculations. *J. Food Sci.* 25, 218-226.
- LENZ, M.K. 1977. The lethality-Fourier number method. Its use in estimating confidence intervals of the lethality or process time of a thermal process and in optimizing thermal processes for quality retention. Ph.D. thesis. Univ. of Wis.—Madison.
- MORE, J.J., GARBOW, B.S. and HILLSTROM, K.E. 1980. User guide for MINPACK-1. Argonne National Laboratory. Argonne, IL.
- OHLSSIN, T. 1980. Optimal sterilization temperatures for sensory quality in cylindrical containers. *J. Food Sci.* 45, 1517-1521.
- OLSON, F.C.W. and JACKSON, J.M. 1942. Heating curves—theory and practical applications. *Ind. Engr. Chem.* 34, 337.
- ÖZİŞİK, M. 1980. Heat conduction. John Wiley & Sons, Inc. New York.
- SINGH, R.P. 1982. Thermal diffusivity in food processing. *Food Technol.* 36(2), 87-91.

- TEIXEIRA, A.A., DIXON, J.R., ZAHRADNIK, J.W. and ZINSMEISTER, G.E. 1969. Computer optimization of nutrient retention in the thermal processing of conduction-heated foods. *Food Technol.* *23*, 137.
- TEIXEIRA, A.A., STUMBO, C.R. and ZAHRADNIK, J.W. 1975. Experimental evaluation of mathematical and computer models for thermal process evaluation. *J. Food Sci.* *40*, 653-655.
- UNO, J. and HAYAKAWA, K. 1979. Nonsymmetric heat conduction in an infinite slab. *J. Food Sci.* *44*, 396-403.
- UNO, J. and HAYAKAWA, K. 1980a. A method for estimating thermal diffusivity of heat conduction food in a cylindrical can. *J. Food Sci.* *45*, 692-695.
- UNO, J. and HAYAKAWA, K. 1980b. Correction factor come-up heating based on critical point in a cylindrical can of heat conduction food. *J. Food Sci.* *45*, 853-859.

APPLICABILITY OF FLOW MODELS WITH YIELD FOR TOMATO CONCENTRATES

M.A. RAO and H.J. COOLEY

Institute of Food Science and
New York State Agricultural Experiment Station
Cornell University
Geneva, New York 14456

Received for Publication December 17, 1981

Accepted for Publication July 22, 1982

ABSTRACT

Shear rate-shear stress data on about fifty tomato concentrates were employed to study the applicability of three flow models: Herschel-Bulkley (H-B), Mizrahi-Berk (M-B), and Vocadlo. The magnitudes of the three parameters of each model were determined by means of nonlinear regression analysis. The H-B and M-B models described very well the flow data. The logarithm of the apparent yield stress values predicted by each model and total solids of the concentrates were related by a quadratic equation. The magnitudes of the flow behavior index of each model did not change significantly over the total solids range studied: 6-36%. The consistency index of the Vocadlo and H-B model, and the concentration of the tomato concentrates were related by a power relationship. Over the temperature range 15-55°C, the flow behavior index of each model did not change significantly. The yield stress decreased with increase in temperature reaching a nearly constant value at 55°C. The consistency index of each model and temperature could be correlated by the Arrhenius equation.

INTRODUCTION

Flow models are used to relate the shear rate and shear stress data of fluid materials. The models can be used in engineering applications such as fluid flow and in transport equations. Some of the flow models are based on the interaction of various components of the foods. For example, the Casson model was derived for suspensions in Newtonian media and the Mizrahi-Berk model was derived for suspensions in non-Newtonian media.

The coefficients of some of the models such as the power law and the model of Casson can be determined via linear regression analysis of the shear rate-shear stress data or their square roots, respectively. In

contrast, in the case of several models containing a yield term linear methods can be used only when the magnitude of yield stress can be determined experimentally.

Yield stress is a desirable property of fluid foods such as tomato pastes and chocolate in food technology applications. However, accurate experimental determination of yield stress can be difficult with many commercial viscometers. For example, the Haake Rotovisco and the Epprecht Rheomat have high moments of inertia (Van Wazer *et al.* 1963). Vocadlo and Charles (1971) pointed out the drawbacks of different experimental methods of determining the yield value and devised a system of concentric cylinders with deep grooves for its accurate determination.

Flow models can be used to determine yield values of fluid foods. For example, the Casson model (Eq. 1) (Casson 1959) has been adopted as the official method for the determination of yield stress by the International Institute of Chocolate. However, recent studies (Mizrahi and Berk 1972; Rao *et al.* 1981) have shown that the Casson model does not fit low shear rate data on concentrated orange juice and tomato concentrates.

$$\tau^{0.5} = K_{OC} + K_C \dot{\gamma}^{0.5} \quad (1)$$

In Eq. (1), τ is the shear stress (N/m²), $\dot{\gamma}$ is the shear rate (s⁻¹), and K_{OC} and K_C are parameters to be determined. The yield stress, τ_0 is equal to K_{OC}^2 .

Nonlinear regression analysis has been found to be useful for evaluating flow models for pharmaceuticals (Niebergall *et al.* 1971) and minced fish paste (Nakayama *et al.* 1980). The objective of the present study was to study the applicability of three models for tomato concentrates by means of nonlinear regression. A related objective was to study the variation of the model parameters with experimental variables, particularly total solids of the foods. The three models studied were: the Herschel-Bulkley (H-B) model (Eq. 2), the Mizrahi-Berk (M-B) model (Eq. 3), and the Vocadlo model (Eq. 4).

$$\tau - \tau_{OH} = K_H \dot{\gamma}^{n_H} \quad (2)$$

$$\tau^{0.5} - K_{OM} = K_M \dot{\gamma}^{n_M} \quad (3)$$

$$\tau = (\tau_{OV}^{1/n_V} + K_V \dot{\gamma})^{n_V} \quad (4)$$

In Eqs. 2-4, all terms other than the shear stress, τ , and the shear rate $\dot{\gamma}$, need to be determined.

Each model contains a yield term. In the case of the M-B model, the yield stress (τ_{OM}) is given by K^2_{OM} . The models have been employed for describing rheological data on food products. The H-B model was employed to describe flow data on protein dispersions (Hermansson 1975) and gum solutions (Balmaceda *et al.* 1973). The M-B model was used to characterize concentrated orange juice (Mizrahi and Berk 1972) and the Vocadlo model was used to characterize commercially available fats (Vocadlo and Moo Young 1969) and mayonnaise (Boger and Tiu 1974). In both the studies on the Vocadlo model (Vocadlo and Moo Young 1969; Boger and Tiu 1974), the parameters K_V and n_V of the model were determined by a trial and error procedure.

Limiting Forms of the Models

Each of the studied models has three parameters that need to be determined. Also, as indicated earlier, each model has a yield term. The H-B model is a modified form of the simple power law model (Eq. 5) with the yield terms, τ_{OH} , added to the simple power law. The M-B model was derived by Mizrahi and Berk (1970, 1972) as a modification of the Casson model (Eq. 1) and it reduces to the Casson model when n_M is equal to 0.5. The Vocadlo model was derived to describe viscoplastic substances (Vocadlo and Charles 1973). It reduces to the simple power law model when τ_{OV} is zero and to the Bingham Plastic model when $n_V = 1$.

MATERIALS AND METHODS

Materials

Four tomato cultivars obtained from the NYS Agricultural Experiment Station farms were used: New Yorker, #475, Nova, and #934. Juice from the tomatoes was obtained using the production line described by Moyer *et al.* (1951) by means of the hot break method. The juice was concentrated to about 15-18% total solids (TS) in a steam-jacketed kettle. Concentrations in the range of 30-36% TS were achieved in a steam-jacketed vacuum kettle equipped with a scraper. Samples of the juice and the concentrates were taken, and intermediate concentrations were obtained by mixing the high solids paste with the juice or a concentrate. The total solids content range of all the concentrates employed in this study was between 5.6 to 36% TS. The magnitude of TS of each concentrate was determined by drying in a vacuum oven at 70°C to a constant weight.

Rheological Data

Shear rate-shear stress data were obtained on about fifty concentrates made from the four experimental tomato cultivars. The data were obtained with a narrow gap (System MVI) concentric cylinder viscometer (Haake, Rotovisco, RV2). Newtonian shear rates calculated from the dimensions of the concentric cylinders were corrected utilizing the magnitude of the slope of log rpm-log shear stress data (Brodkey 1967). Shear stress was calculated from the torque readings using the constants supplied by the manufacturer. Standard fluids (Brookfield Engineering Co.) were used to verify the shear stress and shear rate calculation methods. Most of the data were obtained at $25 \pm 0.1^\circ\text{C}$. In case of concentrates of Nova tomatoes, data were obtained at five temperatures between 15 and 55°C . The temperature of the samples was controlled by means of a circulating bath (Lauda, K-2/R).

A 50 g-cm torque measuring head was used with concentrates below about 12% total solids and a 500 g-cm torque measuring head was used with concentrates above 12% total solids (up to about 30% total solids). Because of the upper limit of each torque measuring head, data were obtained at relatively high shear rates in the case of concentrates with low and intermediate values of total solids; in the case of concentrates with high total solids, data were obtained over relatively low shear rates. Thus the applicability of the three flow models could be tested using data at high as well as low shear rates.

The applicability of the simple power law (Eq. 5) and the Casson model (Eq. 1), and the effect of concentration on apparent viscosity were reported previously (Rao *et al.* 1981). The magnitudes of the parameters of the power law and Casson models were utilized in the estimation of the initial values of the parameters for the three models in the present study.

$$\tau = K\dot{\gamma}^n \quad (5)$$

In Eq. (5), K is the consistency index and n is the flow behavior index.

Nonlinear Regression Analysis

The parameters of the three models (Eqs. 2-4) were estimated by nonlinear regression analysis. The computer program of Niebergall *et al.* (1971) was adapted for each flow model. The partial derivatives of shear stress (the square root of shear stress in the case of M-B model) with respect to each model parameter were entered in a subroutine of the program in order to estimate the correction vectors for the parameters. The computations were performed on a Prime 400 digital computer.

For each model, the initial values of the parameters were crucial for the program to perform several iterative calculations. For the H-B model, the initial values of the flow behavior index and the consistency index were estimated using the Casson yield stress and linear regression analysis of Eq. 2. For the Vocadlo model, initial values of n_V and τ_{OV} were those from the H-B model. Initial values of K_V estimated at the high end or middle of the shear rate-shear stress data were satisfactory; in contrast, at the low end of the data the magnitudes of K_V were negative. For the M-B model, the initial values of K_{OM} were the square roots of τ_{OH} of the H-B model and n_M was assumed to be 0.480 for reasons to be discussed later. The initial magnitudes of K_M were estimated in the middle of the shear rate-shear stress data.

With each model, the regression analysis program was run three times. The results from one run were employed as the initial values for the next run. The magnitudes of the parameters of each model from the second and third runs did not differ in the first place after the decimal.

RESULTS AND DISCUSSION

Applicability of the Models

The applicability of the three models to the two sets of data on Nova concentrates, selected arbitrarily, is illustrated on rectangular coordinates in Fig. 1-3. Rectangular coordinates were employed because with log-log coordinates deviations between experimental data and predictions of the models will not be as discernible. The shear rate range of the data on 16.8 total solids (TS) concentrate is 20–1,370 s^{-1} and that for 28.8 TS concentrate is 0.25–12.5 s^{-1} . In general, as seen in Fig. 1-3, the three models can be used to describe the flow data over both narrow and wide ranges of shear rates.

The H-B and M-B models follow well both sets of data in the low shear rate range. In contrast, the Vocadlo model bypasses data in the low range of shear rates and predicts values of yield stress higher than the other two models. The sum of the squares of the residuals of the experimental and predicted values was higher in the case of the Vocadlo model than for the H-B and M-B models. For the 16.8 TS concentrate, the sums of squares of the residuals were 227, 557, and 652 for the H-B, M-B, and Vocadlo models, respectively; the corresponding figures for the 28.8 TS concentrate were 381, 439, and 1,066, respectively.

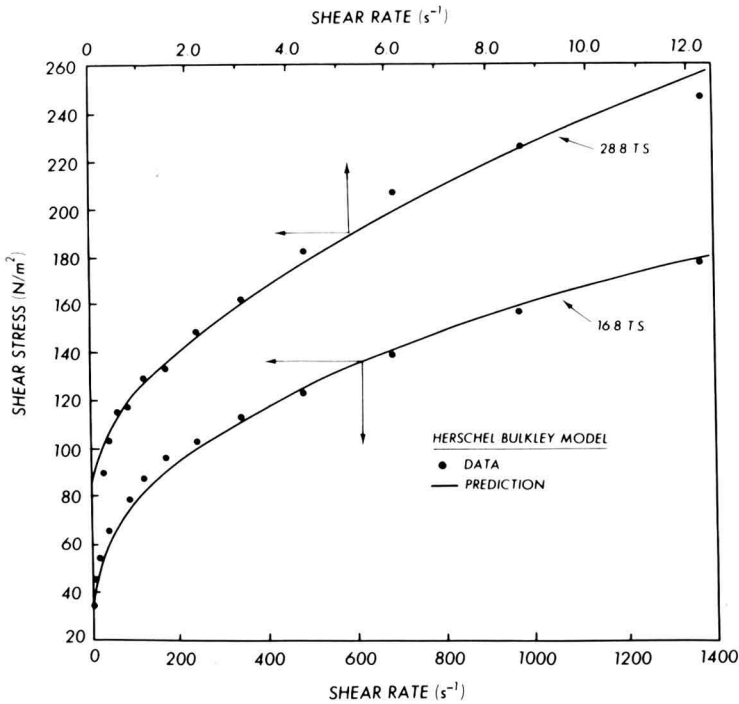


FIG. 1. APPLICABILITY OF THE HERSCHEL-BULKLEY MODEL

Relationship Between Yield Stress and Concentration

The H-B and Vocadlo models provide directly magnitudes of yield stress τ_{OH} and τ_{OV} , respectively. In the case of the M-B model, the yield stress was calculated as the square of K_{OM} ($\tau_{OM} = K_{OM}^2$). Regression analysis of total solids and yield stress data indicated the relationship between the two quantities can be described by Eq. (6).

$$\ln \tau_O = a + b(TS) + c(TS)^2 \quad (6)$$

The magnitudes of the constants a , b , and c for τ_{OH} , τ_{OM} , and τ_{OV} are in Tables 1, 2, and 3, respectively. Because the magnitude of c is negative in all cases, yield stress increases with total solids at slightly less than an exponential rate. Figure 4 shows τ_{OV} and τ_{OM} for #475 tomato concentrates as a function of total solids; for the sake of clarity, τ_{OH} was not included in the figure. Correlation coefficients for exponential and power type relationships between yield stress and total solids were lower than those listed in Tables 1-3.

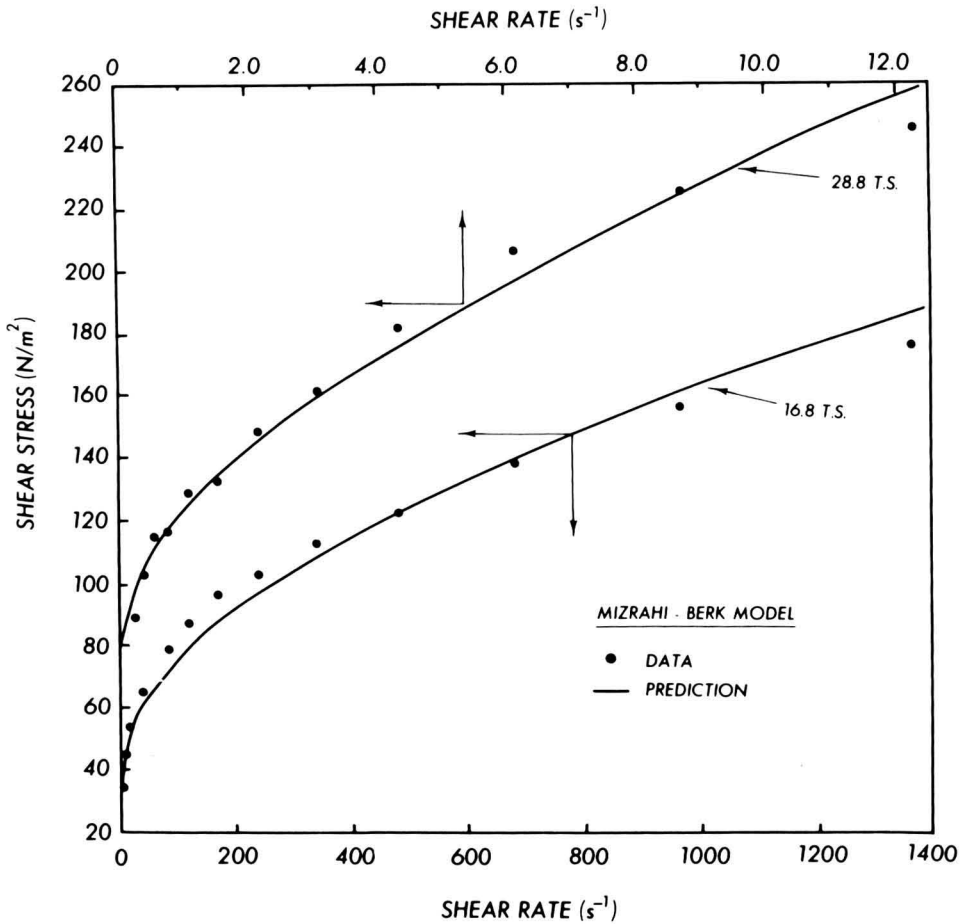


FIG. 2. APPLICABILITY OF THE MIZRAHI-BERK MODEL

It is emphasized that Eq. (6) must be used to estimate the yield stress values predicted by a model at realistic values of total solids. This is important because the relationship (Eq. 6) does indicate non-zero yield stress values at zero concentration (TS) due to its empirical nature. Likewise, even though the models predict yield stress values at low magnitudes of TS it is doubtful that such values can be discerned in experiments.

The coefficients in Tables 1-3 can be used to calculate the magnitudes of yield stress predicted by each model from the total solids content of a concentrate. For example, in the case of a #475 tomato concentrate with 30% TS the magnitudes of H-B yield stress, M-B yield stress, and

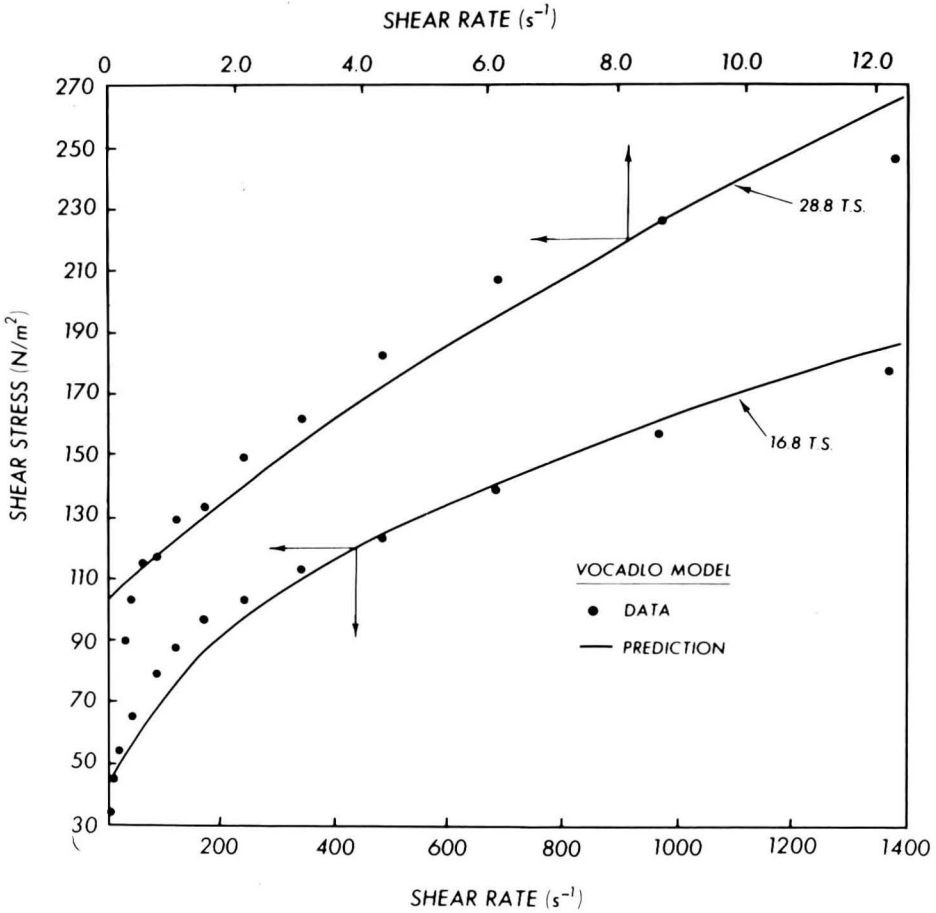


FIG. 3. APPLICABILITY OF THE VOCADLO MODEL

Vocadlo yield stress are 109 N/m², 102 N/m², and 131 N/m², respectively. As indicated earlier, the Vocadlo model bypasses data at low shear rates and predicts relatively high values of yield stress. It is interesting

Table 1. Magnitudes of constants in the relationship between total solids and H-B yield stress: $\ln \tau_{OH} = a + b(TS) + c(TS)^2$

Tomato Variety	<i>a</i>	<i>b</i>	<i>c</i>	r^2
#934	-0.4471	0.2152	-0.00200	0.900
#475	0.8639	0.1835	-0.00186	0.970
Nova	-0.6443	0.3652	-0.00645	0.957
New Yorker	-0.1642	0.2219	-0.00248	0.890

Table 2. Magnitudes of constants in the relationship between total solids and M-B yield stress: $\ln \tau_{OM} = a + b(\text{TS}) + c(\text{TS})^2$

Tomato Variety	<i>a</i>	<i>b</i>	<i>c</i>	<i>r</i> ²
#934	-0.3911	0.2061	-0.00177	0.891
#475	0.7261	0.2025	-0.00242	0.942
Nova	-0.9710	0.4102	-0.00777	0.972
New Yorker	-0.0499	0.1926	-0.00162	0.865

to note that the yield stress estimated by each model for #475 tomato is higher than for the other varieties and this is reflected in the positive value of the coefficient *a* in Eq. (6).

Relationship Between K_H , K_M , and K_V and Total Solids

The total solids of the concentrates and the parameters K_H and K_V were well correlated by a power type relationship:

$$K_i = \alpha(\text{TS})^\beta \quad (7)$$

The correlation coefficients for the power type relationship were found to be higher than those for an exponential relationship. The magnitudes of α and β for the H-B and Vocadlo models are in Tables 4 and 5, respectively. It is readily seen that the magnitudes of β for K_V are higher than those for K_H due to the relatively high magnitudes of K_V . For example, the magnitudes of K_H and K_V for a 30% TS concentrate made from #475 tomatoes are 46 N.s^{n_H}/m² and 1,950 (N.s^{n_V}/m²)^{1/n_V}. Vocadlo and Moo Young (1969) and Boger and Tiu (1974) also reported very large values of K_V for fats and mayonnaise. Thus, relatively large values of K_V is another characteristic of the Vocadlo model.

The parameter K_M of the M-B model also increased with increase in TS but the increase was not as large as for K_H and K_V . The magnitudes of α and β in Eq. 7 for K_M are in Table 6 and it is seen that the magnitudes of β are lower than those for K_H and K_V . Also, the magnitudes of r^2 are lower than those for K_H and K_V . Mizrahi and

Table 3. Magnitudes of constants in the relationship between total solids and Vocadlo yield stress: $\ln \tau_{OV} = a + b(\text{TS}) + c(\text{TS})^2$

Tomato Variety	<i>a</i>	<i>b</i>	<i>c</i>	<i>r</i> ²
#934	-0.0990	0.2050	-0.00178	0.903
#475	0.8851	0.2078	-0.00249	0.970
Nova	-0.3774	0.3683	-0.00665	0.937
New Yorker	0.2528	0.1914	-0.00162	0.885

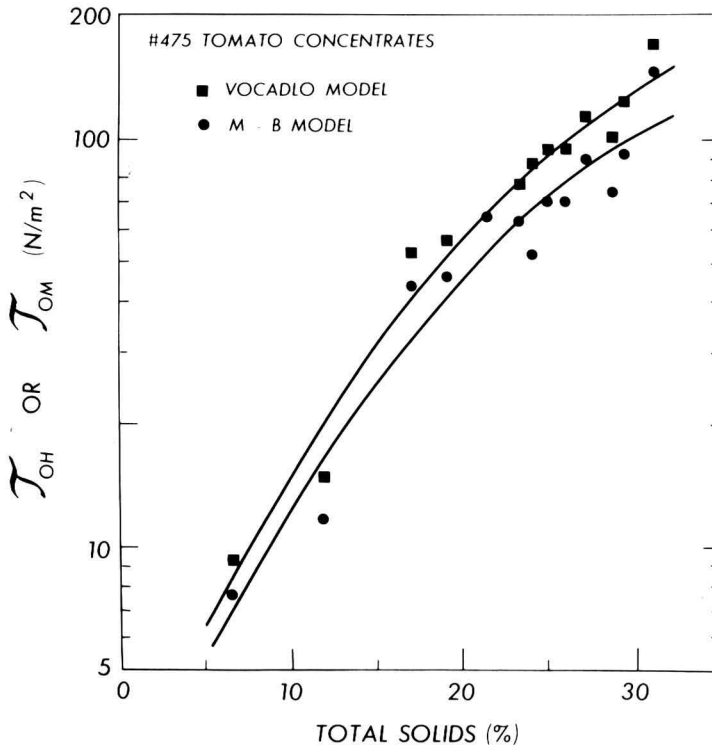


FIG. 4. RELATIONSHIP BETWEEN YIELD STRESS (N/m^2) VALUES PREDICTED BY THE MIZRAHI-BERK AND VOCADLO MODELS, AND CONCENTRATION OF #475 TOMATO CONCENTRATES

Firstenberg (1975) showed that for concentrated orange juice K_M can be correlated with the pulp content and the relative viscosity of the serum. In the present study, the serum viscosity of the tomato concentrates was not determined so that observations of Mizrahi and Firstenberg (1975) could be confirmed.

Table 4. Magnitudes of the parameters α and β in Eq. 7 for K_H of the H-B model

Tomato Variety	α	β	r^2
#934	3.08×10^{-3}	2.45	0.839
#475	1.48×10^{-3}	3.04	0.941
Nova	3.60×10^{-4}	3.37	0.932
New Yorker	4.73×10^{-3}	2.28	0.723

Table 5. Magnitudes of the parameters α and β in Eq. 7 for K_V of the Vocadlo model

Tomato Variety	α	β	r^2
#934	1.3×10^{-5}	5.02	0.849
#475	2.8×10^{-5}	5.31	0.908
Nova	9.6×10^{-7}	6.20	0.907
New Yorker	5.7×10^{-4}	3.64	0.595

Relationship Between n_H , n_M , and n_V and Total Solids

The magnitudes of the parameters n_H , n_M , and n_V did not vary significantly over the range of concentrations studied. The mean values of n_H , n_M , and n_V and their standard deviations are in Table 7. Because their magnitudes are less than 1.0, the concentrates are shear-thinning (pseudoplastic) fluids.

The M-B model was developed for suspensions in shear-thinning media (Mizrahi and Berk 1972) with $n_M < 0.5$. For suspensions in Newtonian media n_M has the maximum value of 0.5 and the M-B model reduces to the Casson model (Eq. 1). The magnitude of n_M for the studied concentrates was less than 0.5 in agreement with the concept that tomato concentrates are suspensions in shear-thinning media. The shear-thinning nature of the serum can be attributed to dissolved pectins. The nonlinear regression program was also employed with n_M values greater than 0.5. It was found that the sum of the squares of the

Table 6. Magnitudes of the parameters α and β in Eq. 7 for K_M of the M-B model

Tomato Variety	α	β	r^2
#934	1.45×10^{-2}	1.15	0.439
#475	2.14×10^{-3}	2.08	0.794
Nova	9.41×10^{-4}	2.20	0.801
New Yorker	1.31×10^{-2}	1.19	0.451

Table 7. Magnitudes of mean values of n_H , n_M , and n_V and their standard deviations

Variety	n_H	σ	n_M	σ	n_V	σ
#934	0.510	0.052	0.457	0.012	0.512	0.050
#475	0.528	0.084	0.454	0.022	0.545	0.061
Nova	0.544	0.061	0.450	0.002	0.540	0.062
New Yorker	0.522	0.066	0.458	0.008	0.531	0.052

difference between the experimental data and the values predicted by regression analysis was lower than n_M was < 0.5 than when n_M was > 0.5 ; similar observation was made by Mizrahi and Firstenberg (1975) in the case of concentrated orange juice.

Effect of Temperature on the Parameters of the Models

The effect of temperature on the parameters of the models was investigated for the shear rate-shear stress data of a 16.7 TS concentrate made from Nova tomatoes over the temperature range 15-55°C. The parameters n_H , n_M , and n_V were nearly constant over the temperature range with mean values of 0.405 ($\sigma = 0.017$), 0.442 ($\sigma = 0.034$) and 0.442 ($\sigma = 0.034$), respectively; the corresponding standard deviations are given in the parenthesis.

The parameters K_H , K_M , and K_V decreased in magnitude with increase in temperature. An Arrhenius type relationship was found to describe the relationship between temperature (°K) and the parameters:

$$K_i = A \exp(E_a/RT) \quad (8)$$

The magnitudes of A , E_a , and r^2 for each parameter are given in Table 8. It is seen that the magnitude of E_a is the highest for K_V and the lowest for K_M , indicating the relative sensitivity of the parameters to temperature.

The parameters τ_{OH} , τ_{OM} , and τ_{OV} decreased rapidly between 10°C and 35°C (Fig. 5). Between 35°C and 55°C, they decreased relatively slowly and it appears the magnitudes have reached nearly constant values. Because of the scatter in the estimated values of the parameters, no attempt was made to fit equations to the curves in Fig. 5. From the shape of the curves, if more data are available, one could employ equations that describe exponential decay with an equilibrium value.

These results are based on data over a limited range of temperatures and additional work is required to confirm these findings. The results have been presented here with the hope that they will provide at least

Table 8. Effect of temperature on K_H , K_M , and K_V ; magnitudes of A and E_a of Eq. (8)

Parameter	A	E_a (kcal/g mole)	r^2
K_H	0.2733	1.955	0.722
K_M	1.290×10^{-3}	3.224	0.415
K_V	1.744×10^{-9}	15.116	0.932

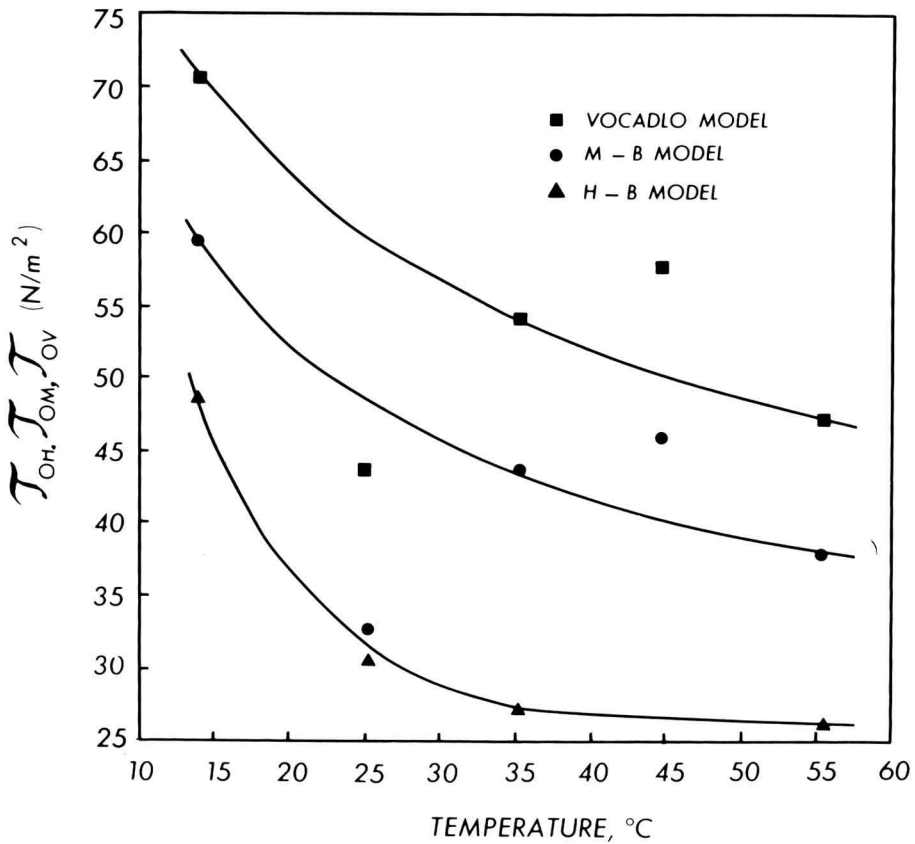


FIG. 5. EFFECT OF TEMPERATURE ON THE MAGNITUDES OF YIELD STRESS (N/m^2) OF A 16.7 TS NOVA CONCENTRATE

the functional relationships that are necessary in engineering studies such as pasteurization of viscous fluid foods (Guariguata *et al.* 1979).

CONCLUDING REMARKS

Nonlinear regression analysis permitted the direct determination of parameters of the three flow models. In particular, the estimation of yield stress by each model is one of the advantages of the analysis. It is emphasized that the predicted values of yield stress are extrapola-

tions of the shear rate-shear stress data of the concentrates and that they are not magnitudes of the physical yield phenomena of the concentrates.

In the case of Vocadlo model, a trial and error procedure has been employed in the past (Boger and Tiu 1974; Vocadlo and Moo Young 1969) to determine magnitudes of K_V and n_V after determining experimentally τ_{OV} ; with the nonlinear regression, a trial and error procedure is not necessary.

Even though the three models followed the shear rate-shear stress data on the concentrates, the Vocadlo model did not describe well data at low shear rates. In terms of yield stress values, the M-B model predicted yield values intermediate to those predicted by H-B and Vocadlo models. The magnitudes of yield stress increased with increase in total solids at less than an exponential rate. The magnitudes of K_V of the Vocadlo model were much higher than either K_H or K_M . The magnitudes of the parameters n_H , n_M , and n_V were relatively constant over the studied range of total solids. Either the H-B or the M-B model can be used to describe accurately the flow data of tomato concentrates.

The limited data on the effect of temperature show that the Arrhenius relationship can be used to relate temperature and the parameters K_V , K_M , and K_H . The parameters n_V , n_H and n_M did not change significantly with temperature. The yield stress values predicted by the models decreased with temperature, reaching nearly constant values at about 55°C.

ACKNOWLEDGMENTS

The authors are deeply indebted to Professor M. C. Bourne for suggesting a previously published study on the rheology of tomato concentrates which generated the ideas for the present study. Mr. Aaron M. Pool provided invaluable assistance with programming a digital computer.

REFERENCES

- BALMACEDA, E., RHA, C-K. and HUANG, F. 1973. Rheological properties of hydrocolloids. *J. Food Sci.* 38, 1169-1173.
- BOGER, D.V. and TIU, C. 1974. Rheological properties of food products and their use in the design of flow systems. *Food Technol. in Australia* 26, 325-335.
- BRODKEY, R.S. 1967. *The Phenomena of Fluid Motions*, Addison-Wesley, Reading, Mass.

- CASSON, N. 1959. A flow equation for pigment-oil suspensions of the printing ink type. In *Rheology of Disperse Systems*, (C.C. Mill, ed.), pp. 82-104. Pergamon Press, New York.
- GUARIGUATA, C., BARREIRO, J.A. and GUARIGUATA, G. 1979. Analysis of continuous sterilization process for Bingham Plastic fluids in laminar flow. *J. Food Sci.* *44*, 905-910.
- HERMANSSON, A.-M. 1975. Functional properties of proteins for foods-flow properties. *J. Texture Studies* *5*, 425-439.
- MIZRAHI, S. and BERK, Z. 1970. Flow behaviour of concentrated orange juice. *J. Texture Studies* *1*, 342-355.
- MIZRAHI, S. and BERK, Z. 1972. Flow behaviour of concentrated orange juice: mathematical treatment. *J. Texture Studies*, *3*, 69-79.
- MIZRAHI, S. and FIRSTENBERG, R. 1975. Effect of orange juice composition on flow behaviour of six-fold concentrate. *J. Texture Studies* *6*, 523-532.
- MOYER, J.C., HOLGATE, K.C., LABELLE, R.L. and HAND, D.B. 1951. Tomato juice line. *Ind. Eng. Chem.* *43*, 1874-1880.
- NAKAYAMA, T., NIWA, E. and HAMADA, I. 1980. Pipe transportation of minced fish paste. *J. Food Sci.* *45*, 844-847.
- NIEBERGALL, P.J., SCHNAARE, R.L. and SUGITA, E.N. 1971. Nonlinear regression applied to non-Newtonian flow. *J. Pharm. Sci.* *60*, 1393-1402.
- RAO, M.A., BOURNE, M.C. and COOLEY, H.J. 1981. Flow properties of tomato concentrates. *J. Texture Studies* *12*, 521-538.
- VAN WAZER, J.R., LYONS, J.W., KIM, K.Y. and COLWELL, R.E. 1963. *Viscosity and Flow Measurement*, Interscience, New York.
- VOCADLO, J.J. and CHARLES, M.E. 1971. Measurement of yield stress of fluid-like viscoplastic substances. *Can. J. Chem. Eng.* *49*, 576-582.
- VOCADLO, J.J. and CHARLES, M.E. 1973. Characterization and laminar flow of fluid-like viscoplastic substances. *Can. J. Chem. Eng.* *51*, 116-121.
- VOCADLO, J.J. and MOO YOUNG, M. 1969. Rheological properties of some commercially available fats. *Can. Inst. Food Technol. J.* *2*, 137-140.

LITERATURE ABSTRACTS

AIChE ABSTRACTS

The Growth of Competing Microbial Populations in a CSTR with Periodically Varying Inputs. G. Stephanopoulos, A.G. Fredrickson, R. Aris. *AIChE Journal* 25, 863. 1979.

The operation of a periodically forced chemostat (CSTR) in which two microbial populations compete for the same nutrient has been examined. Easily implemented criteria for the stability of the resulting cycles have been obtained, using the Floquet stability theory. After examining several possibilities it was found that stable periodic trajectories of coexistence can be achieved: (a) when the dilution rate of the chemostat is properly varied in a periodic manner between two values so chosen that the growth of one population is favored by the first and the growth of the other population is favored by the second, (b) when a certain percentage of biomass and growing medium is harvested periodically from the chemostat, and (c) when both the dilution rate and the concentration of the substrate in the feed are varied simultaneously and in a periodic manner.

Growth of Ice in a Saltwater Drop Falling in an Organic Phase. S.T. Bustany, P. Harriott, H.F. Wiegandt. *AIChE Journal* 25, 439. 1979.

Data on the ice formation rate are presented for a saltwater drop suspended by drag forces in a flowing cold organic liquid. The effects of refrigerant undercooling, salt concentration, drop size, and time were studied. Ice formation rates in drops of 3 wt % sodium chloride solution were two to three times lower than in pure water drops. A parallel plate model was used to correlate the data and predict ice formation rates for other drops and refrigerants.

Dispersing drops of brine or fruit juices in a countercurrent cold organic refrigerant is a method of desalination (or freeze concentration) that deserves further study.

The Mixing of Granular Solids in a Rotary Cylinder. J. Mu, D.D. Perlmutter. *AIChE Journal* 26, 928. 1980.

A model is derived for solids mixing and material transport in a continuous flow rotary dryer or reactor. Detailed analysis of the particle motions in the turnover process provides an opportunity to apply well-known reactor models to several subregions and to relate the overall results to different design geometries and operating conditions. The essential parameters of the model are the number of stages, the volume fractions of mixed flow and plug flow in each stage, the recycle ratio and the bypass ratio.

Separation of Proteins Via Multicolumn pH Parametric Pumping. H.T. Chen, W.T. Yang, U. Pancharoen, R. Parisi. *AIChE Journal* 26, 839. 1980.

Fractionation of protein mixtures by multicolumn pH parametric pumping is investigated theoretically and experimentally. The parapumps considered consist of a series of columns packed alternately with cation and anion exchangers. Various methods of operation of the parapumps are discussed. Two separation problems are examined: enrichment and splitting. Experimental data were obtained for two-column systems and compared with the calculated results based on an equilibrium theory.

Simultaneous Melting and Freezing in the Impingement Region of a Liquid Jet. M. Epstein, M.J. Swedish, J.H. Linehan, G.A. Lambert, G.M. Hauser, L.J. Stachyra. *AIChE Journal* 26, 743. 1980.

An experimental investigation of an impinging water jet freezing on a melting solid surface has been carried out. Attention was focused on the stagnation region of an axisymmetric jet. In the experiment, a water jet was directed upward against the lower end of a meltable rod, having a diameter about twice that of the jet orifice. Solid octane (m.p.—56.5°C) and solid mercury (m.p.—38.9°C) served as the meltable materials. A laminar-axisymmetric flow model was developed to describe melting heat transfer in the presence of jet solidification within the impingement region. Measurements of the melting rate and conditions for the onset of jet solidification were found to agree quite well with the values predicted with this model.

Volatiles Loss During Atomization in Spray Drying. T.G. Kieckbusch, C.J. King. *AIChE Journal* 26, 718. 1980.

Losses of volatile acetates have been measured in the vicinity of pressure nozzles during spraying of sucrose and maltodextrin solutions. Large losses occur very near the atomizer, where only a small portion of the water has evaporated. The effects of atomizer design, nozzle pressure, sucrose concentration, air flow rate, air temperature and liquid feed temperature have all been measured. Correlation of volatiles loss vs. percent water evaporation accounts for most of the effects of changes in spray pattern and drop size distribution. Individual contributions of gas and liquid phase mass transfer are determined from the relative retentions of acetates of different molecular weight and from the effect of sucrose concentration. In the expanding film at the nozzle, both gas and liquid phase resistances are important, but the losses become entirely liquid phase controlled once drops are formed.

Progressive Freezing of Composites Analyzed by Isotherm Migration Methods. *AIChE Journal* 27, 928. 1981.

The Isotherm Migration Method of numerically analyzing conduction with phase change is modified to handle surface and external resistances, appearance, and propagation of successive fronts into slabs of composite material of one or more constituents finely dispersed in a matrix, different components transforming at

different temperatures. Procedures are developed for selecting temperature intervals between isotherms, initially locating isotherms by means of analytical approximations to the earliest stages, and thereafter inserting and removing isotherms as appropriate, particularly when each component gives rise to a separate front.

Bacterial Population Dynamics in Batch and Continuous-Flow Microbial Reactors. Y. Nishimura, J.E. Bailey. *AIChE Journal* 27, 73. 1981.

Calculations of the distribution of states in cell populations grown in well-mixed, isothermal batch and continuous flow reactors are presented. By restricting the analysis to a class of bacteria for which cell division control may be modeled using overlapping timers, analytical results are obtained for many cell population characteristics in terms of the growth rate history. This required growth rate trajectory is evaluated using a separate overall reactor model. The simulation results conform qualitatively to available experimental data and suggest new experiments for further testing of the single-cell model.

An Experimental Investigation of Stability and Multiplicity of Steady States in a Biological Reactor. D. Dibiasio, H.C. Lim, W.A. Weigand. *AIChE Journal* 27, 284. 1981.

The existence of multiple stable and unstable states in a continuous stirred tank biological reactor (CSTBR) was demonstrated experimentally for the first time. These experiments resulted in the determination of growth rate, yield and intermediate metabolite concentration data entirely from continuous culture. This information was used to qualitatively interpret the stability behavior in terms of the biochemistry and bioenergetics of substrate metabolism.

Heat and Mass Transfer in Hygroscopic Capillary Extruded Products. M. Fortes, M.R. Okos. *AIChE Journal* 27, 255. 1981.

This work presents an analysis of heat and mass transfer of extruded corn meal. Isotherm, thermal conductivity, drying and center temperature data were experimentally obtained for the cylindrically extruded product.

Modeling of the drying process was made by incorporating the mechanistic and irreversible thermodynamics approaches for determining heat and mass transfer in capillary-porous media. The proposed model shows that both liquid and vapor fluxes can be expressed in terms of the same driving-forces, namely, temperature and equilibrium moisture content gradients. A search technique allowed for the evaluation of both liquid and vapor conductivities.

Bacterial Film Growth in Adsorbent Surfaces. G.F. Andrews, C. Tien. *AIChE Journal* 27, 396. 1981.

Simultaneous biological and activated-carbon treatment of organic wastewaters appears promising. The effects of bacterial film growth on adsorbent particles is investigated by laboratory work and mathematical modelling. Regeneration of the adsorbent due to film growth does occur, but faster than predicted. The discrepancy reflects uncertainty about the structure of bacterial films.

^N
P

JOURNALS AND BOOKS IN FOOD SCIENCE AND NUTRITION

Journals

- JOURNAL OF NUTRITION, GROWTH AND CANCER, G. P. Tryfiates
JOURNAL OF FOODSERVICE SYSTEMS, O. P. Snyder, Jr.
JOURNAL OF FOOD BIOCHEMISTRY, H. O. Hultin, N. F. Haard and J. R. Whitaker
JOURNAL OF FOOD PROCESS ENGINEERING, D. R. Heldman
JOURNAL OF FOOD PROCESSING AND PRESERVATION, T. P. Labuza
JOURNAL OF FOOD QUALITY, M. P. DeFigueiredo
JOURNAL OF FOOD SAFETY, M. Solberg and J. D. Rosen
JOURNAL OF TEXTURE STUDIES, P. Sherman and M. C. Bourne

Books

- ENVIRONMENTAL ASPECTS OF CANCER: THE ROLE OF MACRO AND MICRO COMPONENTS OF FOODS, E. L. Wynder, G. A. Leveille, J. H. Weisburger and G. E. Livingston
SHELF-LIFE DATING OF FOODS, T. P. Labuza
ANTINUTRIENTS AND NATURAL TOXICANTS IN FOOD, R. L. Ory
UTILIZATION OF PROTEIN RESOURCES, D. W. Stanley, E. D. Murray and D. H. Lees
FOOD INDUSTRY ENERGY ALTERNATIVES, R. P. Ouellette, N. W. Lord and P. E. Cheremisinoff
VITAMIN B₆: METABOLISM AND ROLE IN GROWTH, G. P. Tryfiates
HUMAN NUTRITION, 3RD ED., R. F. Mottram
DIETARY FIBER: CURRENT DEVELOPMENTS OF IMPORTANCE TO HEALTH, K. W. Heaton
RECENT ADVANCES IN OBESITY RESERCH II, G. A. Bray
FOOD POISONING AND FOOD HYGIENE, 4TH ED., B. C. Hobbs and R. J. Gilbert
POSTHARVEST BIOLOGY AND BIOTECHNOLOGY, H. O. Hultin and M. Milner
THE SCIENCE OF MEAT AND MEAT PRODUCTS, 2ND ED., J. F. Price and B. S. Schweigert
THE ROLE OF FOOD PRODUCT DEVELOPMENT IN IMPLEMENTING DIETARY GUIDELINES, G. E. Livingston, C. M. Chang and R. J. Moshy

GUIDE FOR AUTHORS

Typewritten manuscripts in triplicate should be submitted to the editorial office. The typing should be double-spaced throughout with one-inch margins on all sides.

Page one should contain: the title, which should be concise and informative; the complete name(s) of the author(s); affiliation of the author(s); a running title of 40 characters or less; and the name and mail address to whom correspondence should be sent.

Page two should contain an abstract of not more than 150 words. This abstract should be intelligible by itself.

The main text should begin on page three and will ordinarily have the following arrangement:

Introduction: This should be brief and state the reason for the work in relation to the field. It should indicate what new contribution is made by the work described.

Materials and Methods: Enough information should be provided to allow other investigators to repeat the work. Avoid repeating the details of procedures which have already been published elsewhere.

Results: The results should be presented as concisely as possible. Do not use tables and figures for presentation of the same data.

Discussion: The discussion section should be used for the interpretation of results. The results should not be repeated.

In some cases it might be desirable to combine results and discussion sections.

References: References should be given in the text by the surname of the authors and the year. *Et al.* should be used in the text when there are more than two authors. All authors should be given in the Reference section. In the Reference section the references should be listed alphabetically. See below for style to be used.

DEWALD, B., DULANEY, J. T. and TOUSTER, O. 1974. Solubilization and polyacrylamide gel electrophoresis of membrane enzymes with detergents. In *Methods in Enzymology*, Vol. xxxii, (S. Fleischer and L. Packer, eds.) pp. 82—91, Academic Press, New York.

HASSON, E. P. and LATIES, G. G. 1976. Separation and characterization of potato lipid acylhydrolases. *Plant Physiol.* 57, 142—147.

ZABORSKY, O. 1973. *Immobilized Enzymes*, pp. 28—46, CRC Press, Cleveland, Ohio.

Journal abbreviations should follow those used in *Chemical Abstracts*. Responsibility for the accuracy of citations rests entirely with the author(s). References to papers in press should indicate the name of the journal and should only be used for papers that have been accepted for publication. Submitted papers should be referred to by such terms as "unpublished observations" or "private communication." However, these last should be used only when absolutely necessary.

Tables should be numbered consecutively with Arabic numerals. The title of the table should appear as below:

Table 1. Activity of potato acyl-hydrolases on neutral lipids, galactolipids, and phospholipids

Description of experimental work or explanation of symbols should go below the table proper.

Figures should be listed in order in the text using Arabic numbers. Figure legends should be typed on a separate page. Figures and tables should be intelligible without reference to the text. Authors should indicate where the tables and figures should be placed in the text. Photographs must be supplied as glossy black and white prints. Line diagrams should be drawn with black waterproof ink on white paper or board. The lettering should be of such a size that it is easily legible after reduction. Each diagram and photograph should be clearly labeled on the reverse side with the name(s) of author(s), and title of paper. When not obvious, each photograph and diagram should be labeled on the back to show the top of the photograph or diagram.

Acknowledgments: Acknowledgments should be listed on a separate page.

Short notes will be published where the information is deemed sufficiently important to warrant rapid publication. The format for short papers may be similar to that for regular papers but more concisely written. Short notes may be of a less general nature and written principally for specialists in the particular area with which the manuscript is dealing. Manuscripts which do not meet the requirement of importance and necessity for rapid publication will, after notification of the author(s), be treated as regular papers. Regular papers may be very short.

Standard nomenclature as used in the engineering literature should be followed. Avoid laboratory jargon. If abbreviations or trade names are used, define the material or compound the first time that it is mentioned.

EDITORIAL OFFICE: Prof. D. R. Heldman, Editor, Journal of Food Process Engineering, Michigan State University, Department of Food Science and Human Nutrition, East Lansing, Michigan 48824 USA.

CONTENTS

Use of Immobilized Lactase in Processing Cheese Whey Ultrafiltrate
S. ROODPEYMA, C.G. HILL, Jr. and C.H. AMUNDSON, University of Wisconsin, Madison, Wisconsin 113

Error Analysis in Estimating Thermal Diffusivity from Heat Penetration Data
JOHN W. LARKIN and JAMES F. STEFFE, Michigan State University, East Lansing, Michigan 135

Applicability of Flow Models with Yield for Tomato Concentrates
M.A. RAO and H.J. COOLEY, Cornell University, Geneva, New York 159

Literature Abstracts 175